UNIVERSITY OF CALIFORNIA SAN DIEGO

Parietal and Hippocampal Representations of Complex Spatial Paradigms

A dissertation submitted in partial satisfaction of the

requirements for the degree of Doctor of Philosophy

in

Cognitive Science

by

Laura E. Shelley

Committee in charge:

Professor Douglas Nitz, Chair
Professor Andrea Chiba
Professor Seana Coulson
Professor Christina Gremel
Professor Lara Rangel

2022

The Dissertation of Laura E. Shelley is approved, and it is acceptable in quality and form for publication on microfilm and electronically.

University of California San Diego

2022

TABLE OF CONTENTS

LIST OF FIGURES

LIST OF TABLES

ACKNOWLEDGEMENTS

I would like to acknowledge Professor Douglas Nitz for his support as the chair of my committee, and for his help and guidance through truly every part of this process. Without such a mentor I would not have made it this far.

I would like to acknowledge my committee members for their support and advice throughout my time at UCSD.

I would also like to acknowledge the Systems Neuroscience Laboratory for their continued support and feedback, as well as the many undergraduate assistants who spent countless hours helping with rat training and recordings.

Chapter 2, in part, has been published in *Hippocampus,* Shelley, L.E. & Nitz, D.A. (2021). The author of the dissertation is the primary author of this publication.

Chapters 3 and 4, in part, have been published in *Neurobiology of Learning and Memory,* Shelley, L.E., Barr, C. I., & Nitz, D.A. (2022). The author of the dissertation is the primary author of this publication.

They say, “Life is short, and neurophysiology is long,” so it really does take a village. Thank you all.

VITA

2008 Bachelor of Arts, Psychology, University of California Santa Cruz
2013 Master of Arts, Psychology, San Diego State University
2022 Doctor of Philosophy, Cognitive Science, University of California San Diego

PUBLICATIONS

Shelley, L.E., Barr, C.I., & Nitz, D.A. (2022). Cortical and hippocampal dynamics under logical fragmentation of environmental space. *Neurobiology of Learning and Memory, 189*.

Alexander, A.S., Tung, J.C., Chapman, G.W., Conner, A.M., Shelley, L.E., Hasselmo, M.E., & Nitz, D.A. (2022). Adaptive integration of self-motion goals in posterior parietal cortex. *Cell Reports, 38*(10).

Shelley, LE & Nitz, DA (2021). Locomotor action sequences impact the scale of representation in hippocampus and posterior parietal cortex. *Hippocampus, 31*, 677-689.

Alexander, A.S. & Shelley, L.E. (2018). Sleep-stage-dependent hippocampal coordination with cingulate and retrosplenial association cortices. *Journal of Neuroscience*, 38(3), 512-514.

Gracian, E.I., Shelley, L.E., Morris, A.M., & Gilbert, P.E. (2013). Age-related changes in place learning for adjacent and separate locations. *Neurobiology of Aging*, 34(10), 2304-2309.

Maasberg, D.W., Shelley, L.E., & Gilbert, P.E. (2012). Age-related changes in detection of spatial novelty. *Behavioural Brain Research, 228*(2), 447-451.

Maasberg, D.W., Shelley, L.E., Gracian, E. I., & Gilbert, P.E. (2011). Age-related differences in the anticipation of future rewards. *Behavioural Brain Research, 223*(2), 371-375.

ABSTRACT OF THE DISSERTATION

Parietal and Hippocampal Representations of Complex Spatial Paradigms

by

Laura E. Shelley

Doctor of Philosophy in Cognitive Science

University of California San Diego, 2022

Professor Douglas Nitz, Chair

In the following experiments, we sought to examine posterior parietal and hippocampal mapping of complex environments and spatial tasks. Experiment 1 found PPC population activity represented location, locomotor action, and progress through a trajectory, and that PPC and HPC's scale of representation followed the action being performed during traversal of a three-dimensional squared spiral track with stairs, ramps, and corners.

Experiment 2 found that animals could learn to apply a behavioral rule where the correct choice varies depending on which half of the room the choice point is located. All animals could perform at well-above chance levels, and their performance transferred to novel locations. Although overall significantly above chance, accuracy was somewhat

decreased on the first trial of a block, possibly due to increased difficulty of the task on each trial 1 where the track was placed in a new location for a set of trials.

Using the paradigm from Experiment 2, Experiment 3 found that PPC and HPC firing patterns remained anchored with the maze itself across environmental locations, as opposed to differentiating the different room locations in their firing. Furthermore, HPC and PPC firing patterns did not discriminate the upcoming turn choice beyond what could be attributed to differences in the animal's speed and orientation. We propose a model for how the task can be solved at different track locations via a conjunction of HPC-on-track mapping and the differing visual cues at each track location. Lastly, Experiment 3 found that HPC firing differentiated the first trial of a block compared to subsequent trials at a particular location, characterized by overall increased rates and a backward-shift in field location. Such differentiation was consistent with the decreased behavioral accuracy on first trials.

Such studies investigating HPC and PPC representation in complex, abstract paradigms reveal the noteworthy forms by which these two networks work in conjunction to map position and action within allocentric and egocentric frameworks. Such dynamic mapping by these and other related structures can give rise to complex and abstract cognitive phenomena bridging behavior and neural activity into a cohesive experience of an event.

Chapter 1: Literature Review and Introduction to the Present Research

1.1 Introduction

In 1948 Edward Tolman put forth the idea that animals have a mental representation of space that could be relied upon to navigate purposefully through an environment, coining the term 'cognitive map' (Tolman, 1948). This idea directly challenged widely accepted behaviorist stimulus-response theories, which claimed that animals had no internal states, and that all behavior was reflexive and could be explained by reinforcement through environmental experience. Tolman's ideas, controversial among his colleagues at the time for lacking evidence, opened up an avenue for studying possible mechanisms for a cognitive map. Soon after, the hippocampus was implicated in spatial mapping. Lesions were associated with both spatial and episodic memory impairments (Scoville & Milner, 1957; Morris, Garrud, Rawlins, & O'Keefe, 1982) and a neural substrate for a cognitive map was first found in hippocampal 'place cells', neurons whose firing activity is specific to certain locations in a room (O'Keefe & Dostrovsky, 1971). These studies sparked a wave of investigation into the hippocampus and surrounding cortical structures and their implications in spatial cognition. Briefly, findings included 'head direction cells' in the postsubiculum whose firing is specific to heading directions (Taube, Muller, & Ranck, 1990), and medial entorhinal cortex 'grid cells' that exhibit grid-patterned firing fields across an environment (Hafting, Fyhn, Molden, Moser, & Moser, 2005). Even more abstract spatial concepts are evident in route mapping by parietal cortex route-centered cells (Nitz, 2006) and parietal cortex mapping of personal and egocentric spaces (Duhamel, Colby, & Goldberg, 1998; Pouget & Driver, 2000).

Known cognitive processes can be studied at the neuron level of analysis. The patterning found in neural systems, a conjunction of many types of information being registered, gives rise to these cognitive phenomena. Neural findings from the past 40 years provide compelling, if often circumstantial, evidence that what is found at the neuron level can legitimately be interpreted as a mechanism for cognitive processes. Such knowledge can provide the foundation for many applications, including finding remedies for cognitive impairments, creating robots that simulate such behavior, or simply satisfying a scientific curiosity.

Although spatial cognition is currently being studied extensively at the neuron level, there are still many complex and abstract aspects of spatial cognition that have not yet been formally studied in a way that links both the behavioral level and the single neuron level of analysis. The hippocampus and parietal cortex are two areas most heavily implicated in spatial cognition in humans, nonhuman primates, and rodents (Scoville & Milner, 1957; Pouget & Driver, 2000; Avillac, Deneve, Olivier, Pouget, & Duhamel, 2005; O'Keefe & Dostrovsky, 1971; Nitz, 2006; Nitz, 2012; Nitz, 2013). Therefore, the completed work will focus on obtaining behavioral data and neural recordings from these two areas while rats perform different complex spatial tasks. First, a review of known aspects of parietal and hippocampal spatial tuning is necessary.

1.2 Parietal Spatial Tuning

The posterior parietal cortex (PPC) is a sensory integration area that receives input from sensory cortices of different modalities, integrates this information, and projects to other areas (Kolb & Walkey, 1987). This region is distinct from neighboring cortical regions as evidenced by its thalamic inputs that other cortical structures do not

receive (Reep, Chandler, King, & Corwin, 1994). The PPC receives inputs from the lateral dorsal thalamic nucleus, but does not receive input from the dorsal lateral geniculate nucleus which distinguishes it from nearby visual areas (Reep et al., 1994).

Given its location and connectivity, it is reasonable to conclude that PPC integrates sensory information, self-motion information, and positions in space in both internal (egocentric) and external (allocentric) frames of reference (Nitz, 2009). Many studies in non-human primates on parietal cortex spatial mapping, including the parietal reach region (PRR) and the lateral intraparietal area (LIP), have revealed spatial activity in an eye-centered frame of reference where the firing pattern was dependent on the location that a stimulus falls on the retina (Cohen & Andersen, 2002). However, this activity that corresponds to an egocentric, eye-centered frame of reference can be modulated by relative positions of other parts of one's self such as the trunk, head gaze, or position of the hand relative to the eye (Andersen, Essick, & Siegel, 1985; Aglioti, Smania, & Peru, 1999; Karnath, Christ, & Hartje, 1993; Vuilleumier, Valenza, Mayer, Perrig, & Landis, 1999; Pouget & Driver, 2000; Nitz, 2013). Such modulation is called a "gain field" and demonstrates how the parietal cortex can simultaneously use different egocentric frames of reference to map out space.

In addition to a retinotopic reference frame, parietal cortex neurons encode space in other egocentric reference frames in multiple modalities, including locations of tactile and auditory stimuli relative to one's self (Duhamel et al., 1998; Grunewald, Linden, & Andersen, 1999; Linden, Grunewald, & Andersen, 1999). The multimodal nature of parietal spatial mapping is supported by the multimodal nature of behavioral deficits in patients with unilateral spatial neglect (Pouget & Driver, 2000).

In addition to activity tuned to various egocentric reference frames, PPC can map one's position in space using an allocentric frame of reference. Posterior parietal cortex neuron activity that occurs at a specific egocentric behavior (such as a left turn) can be modulated depending on its order in a complex route, a type of allocentric reference frame (Nitz, 2006). This route-centered activity seems to integrate with the spatial activity based on an egocentric reference frame to map out position in an entire route, or even map out position within parts of a route, effectively mapping out parts of a space into a whole and forming a continuity between the route segments (Nitz, 2006; 2012; 2013).

This modulation of internal reference frame information by action sequences in an external frame of reference is analogous to the gain fields studied in non-human primates (described above). However, in primate studies, the animals are usually head-fixed, effectively clamping the vestibular system. Studying this area in the freely behaving rat affords us the advantage of being able to investigate how self-motion through an environment can modulate PPC firing activity, as vestibular input may have an impact on PPC activity (Nitz, 2013). Additionally, the PPC also interacts with the hippocampal formation (Rogers & Kesner, 2007), and studying a freely moving rat may allow that hippocampal spatially specific firing information to interact with PPC mapping of space.

1.3 Hippocampal Spatial Tuning

In contrast to the parietal cortex, the hippocampus contains place cells with firing activity that is specific to certain spatial locations in relation to the external environment, an allocentric frame of reference (O'Keefe & Dostrovsky, 1971). In other words, a place cell will fire when a rat is in a specific location within a room. The location of a

particular neuron's place field is anchored to the boundaries of the environment, such that if you shift or rotate landmarks or cues on the walls, the field location moves accordingly (Muller & Kubie, 1987). This is a different, but complementary type of allocentric reference frame than that of the PPC as described above. This basic allocentric firing activity that is characteristic of the HPC can be modified by various features of the environment, including the trajectory the animal takes through the space (Frank, Brown, & Wilson, 2000; Ferbinteanu & Shapiro, 2003; Nitz, 2011). This trajectory-dependent modulation has implications for how the hippocampus might play a role in forming episodic memories as an animal moves through a space (Nitz, 2011).

1.3.1 Trajectory Encoding and Episodic Memory

The HPC in humans is critical for the generation of new episodic memories (Scoville & Milner, 1957). Traveling along a path can be thought of as an "episode" in that it entails a series of ordered events defined by the combination of the animal's actions and sensory experiences. Accordingly, action sequences and trajectory shapes are critical components of spatial mapping. Trajectory-specific encoding is a phenomenon associated with altered in-place-field firing rates of HPC neurons depending on the full trajectory taken to reach those place fields or taken subsequent to those place fields (Ferbinteanu & Shapiro, 2003). Trajectory and action-specific encoding exists in other forms as well. For instance, place cells are direction-sensitive (McNaughton, Barnes, & O'Keefe, 1983; Markus et al., 1995), but much more so when the animal runs on a track completing a task defined by specific actions rather than free-foraging (Markus et al., 1995).

Path shape can also impact the scale and recursion of HPC firing fields. For instance, Nitz (2011) found CA1 cell firing patterns of spiral tracks tend to recur in locations of the tracks that were spatially similar (i.e. analogous segment positions across loops of a spiral, where similar actions were required for traversal). Additionally, firing fields of some place cells were elongated on straight portions of the longer loops. If the HPC firing pattern generalizes across similar spaces, then it stands to reason that the episodic memory for that sequence of actions is likely similar. Thus, how an animal moves through space is directly related to spatial mapping, potentially explaining HPC's roles in spatial mapping and episodic memory.

Episodes are also encoded in HPC firing patterns via "theta phase precession", a neural coding phenomenon where the animal's past, current, and expected future positions (Lubenov & Siapas, 2009) organize the spiking order of HPC place cells whose place field centers lie in the past, present, and future. Such organized spiking occurs over the phases of prominent theta-frequency (5-10 Hz) oscillations seen in the HPC local field potential (O'Keefe & Recce, 1993). HPC place cell action potentials 'phase precess,' in that spiking for any given cell occurs at late phases as the animal enters the cell's place field, at peak (middle) phases when the animal passes the center of the field, and at early phases near the exit of the field. As a consequence, across an entire trajectory and HPC cell population, neuronal firing repeatedly represents where the animal is, where he's just been, and where he's going. The phenomenon is considered critical to learning of new episodic memories in that: 1) the spiking order reflects the ordering of the animal's experience while running down the path and 2) the timing of spikes is consistent with spike timing dependent plasticity rules governing learning processes in

the HPC (Bi & Poo, 2001). Thus, HPC activity patterns reflect space as well as the full episode of places visited along a trajectory. Yet, how HPC spiking activity relates to vertically-going action sequences and trajectories has not been determined. Furthermore, there is scarce knowledge concerning how different forms of information associated with an environmental experience are integrated in HPC and how specific connectivity patterns within HPC and between HPC and other structures may support such integration.

1.4 Complementary Spatial Mapping by Parietal and Hippocampal Neurons

With respect to mapping positional relationships between an organism and its environment, the HPC and PPC in rodents, nonhuman primates, and humans are key structures. In each of these species, lesions in these structures produce profound impairments in spatial cognition and navigation, and neurons in these regions robustly map spatial relationships in their firing rates. In addition, when navigating along pathways through an environment, the HPC and PPC generate different forms of spatial mapping (e.g. they encode position in different reference frames), but these different forms play complementary roles in navigation (Nitz, 2012; Nitz, 2006; Rogers & Kesner, 2007). The rat HPC maps, in its ensemble firing patterns position within the environment (O'Keefe & Dostrovsky, 1971), while the PPC maps position within the space of a route irrespective of that route's position in the environment (Nitz, 2006). These distinct forms of spatial mapping are complementary in the way they transition spatial cognition into navigational actions.

1.5 The Present Research

The present research seeks to examine parietal and hippocampal dynamics in representing complex environments and spatial tasks. Experiment 1 will evaluate parietal

and hippocampal neurons role in mapping out locomotor action sequences in a complex, three-dimensional squared-spiral maze, and the impact those locomotor actions have on the scale of representation. Experiment 2 will evaluate rat's behavioral performance in a decision-making task that is dependent on a logical subspacing of an environment. Experiment 3 will evaluate the role of hippocampal and parietal neurons in representing the subspaces created in Experiment 2.

Chapter 2: Experiment 1 – Locomotor Action Sequences Impact the Scale of Representation in Hippocampus and Posterior Parietal Cortex

2.1 The Present Study

The hippocampus (HPC) and posterior parietal cortex (PPC) in both rats and humans are brain structures implicated in spatial navigation and the generation of new episodic memories (Scoville & Milner, 1957; Ergorul & Eichenbaum, 2004; O'Keefe & Dostrovsky, 1971; Muller & Kubie, 1987; Benoit & Schacter, 2015; Saj, Fuhrman, Vuilleumier, & Boroditsky, 2014; Hassabis, Kumaran, & Maguire, 2007; Rogers & Kesner, 2007). Episodic memory formation, while dependent on HPC, nevertheless appears to be a process distributed across multiple brain regions (Hassabis et al., 2007). Accordingly, HPC, PPC, and retrosplenial cortex all share a common temporal framework for activity based on the hippocampal theta rhythm (8 Hz) (O'Keefe & Recce, 1993; Sirota et al., 2008; Alexander, Rangel, Tingley, & Nitz, 2018). Such temporal organization is considered critical to learning new episodic memories in that spike ordering according to the phase of theta frequency oscillations is thought to drive alterations in synaptic efficacy (Pavlides, Greenstein, Grudman, & Winson, 1988; Huerta & Lisman, 1993; O'Keefe & Recce, 1993; Skaggs, McNaughton, Wilson, & Barnes, 1996). These alterations are thought to form the basis for a physical instantiation of distributed episodic memory.

Spatial tuning of activity in HPC presents itself in the form of place-specific spiking in individual neurons that carries the reference frame of environmental boundaries (O'Keefe & Dostrovsky, 1971; Muller & Kubie, 1987). Yet place-specific activity is robustly modulated by the trajectory the animal takes through space, producing

different patterns for different trajectories through the same location (Ferbinteanu & Shapiro, 2003; McNaughton, Barnes, & O'Keefe, 1983; Markus et al., 1995; Frank, Brown, & Wilson, 2000; Wood, Dudchenko, Robitsek, & Eichenbaum, 2000; Ainge, Tamosiunaite, Woergoetter, & Dudchenko, 2007; Grieves, Wood, & Dudchenko, 2016). In principle, this allows differentiation in memory of otherwise distinct trajectory-running episodes that pass through the same space and reconciles the contradiction between pure spatial mapping and pure episodic memory formation functions proposed for HPC. In complement to this, the same trajectory taken through different places can produce recursion in the population firing patterns for different environmental locations (Nitz, 2011; Singer, Karlsson, Nathe, Carr, & Frank, 2010). To the extent that HPC population firing patterns reflect the content of episodic memories, such recursion would result in some degree of generalization across memories for the same trajectories taken through different locations in the environment.

In complement to HPC place-specific activity, PPC neurons often have action correlates that effectively map locomotor sequences accompanying movement through specific trajectories (Mimica, Dunn, Tombaz, Bojja, & Whitlock, 2018; Nitz, 2006; McNaughton et al., 1994; Wilber, Clark, Forster, Tatsuno, & McNaughton, 2014; Whitlock, Pfuhl, Dagslott, Moser, & Moser, 2012). Such action correlates are often strongly and reliably modulated by the location of those actions within a trajectory (Nitz, 2012; McNaughton et al., 1994; Whitlock et al., 2012; Wilber et al., 2014). Furthermore, PPC neurons lacking action correlates exhibit reliable spatial tuning to progress through trajectories of a particular shape irrespective of the environmentally-defined locations and directions of travel associated with them (Nitz, 2006; Nitz, 2012). In this sense, the PPC

forms a map both for specific locomotor actions and for location in a trajectory, or route. Thus, trajectory modulates both place-specific activity in the HPC and action-related activity in PPC and represents a common spatial framework by which to examine how locations and actions can be registered within the same episodic memories.

Although there are reports of actions at a given location modulating the place-specific activity of HPC neurons (Aghajan et al., 2015; Markus et al., 1995), it is unclear how extensively the trajectory-modulated place-specific activity in HPC and trajectory-modulated action-specific activity in PPC are coordinated. This is relevant because any episodic memory for a path taken through the world is more than just a memory for a series of visited locations. Episodic memories for completion of a trajectory will typically include the locomotor actions performed during traversal. Indeed, such inclusion is arguably critical to generating memories for repeatedly used paths between environmental locations. Therefore, understanding how trajectory-modulated action and location tuning in PPC and HPC relate would provide a better understanding of the distributed components of episodic memory generation.

To more thoroughly examine the impact of trajectory on HPC place coding and PPC action coding, the current study utilized a five-loop, squared spiral track that extends the array of sampled locomotor actions beyond left and right turning to include actions such as stair-hopping and ramp-running that move the animal in the vertical dimension. The full track length is composed of recurring trajectories in the form of individual 'loops' that pass through different allocentric locations in the recording room. Such trajectory recurrence is known to modulate action-specific activity in PPC and place-specific activity in HPC (Nitz, 2011; Nitz, 2012) and is therefore a tool by which to

examine coordinated alterations of spatially tuned firing in HPC and PPC. Further, the expanded range of locomotor actions on the part of the animal provides a methodology to better understand how actions are mapped into activity patterns of HPC and PPC. Notably, prior work suggests that movement in the vertical dimension is mapped in a qualitatively different way than for horizontal dimensions. In HPC and medial entorhinal cortex, tuning according to the vertical dimension is degraded relative to the horizontal dimensions (Hayman, Verriotis, Jovalekic, Fenton, & Jeffery, 2011; Hayman, Casali, Wilson, & Jeffery, 2015; Casali, Bush, & Jeffery, 2019; Porter, Schmidt, & Bilkey, 2018). Place cells on a flat surface exhibit partial remapping once the surface is tilted vertically (Knierim & McNaughton, 2001; Porter et al., 2018). Anterodorsal thalamic head direction cells maintain their tuning specific to prior, horizontally-defined orientations when the animal traverses horizontal corners and begins to climb vertically (Taube, Wang, Kim, & Frohardt, 2013), and shift their tuning 90 degrees when the animal traverses vertical corners (LaChance, Dumont, Ozel, Marcroft, & Taube, 2020). Actions associated with movement in the vertical dimension (e.g., stair-hopping or jumping) are often qualitatively distinct from those associated with movement in the horizontal dimensions. In principle then, the incorporation of action-tuned activity into episodic memories could serve to provide key information regarding the presence or absence of vertical dimension movement in episodic memories for trajectories. Thus, the current experiments involve different forms of vertical behaviors including stair hopping, locomotion on an incline, and transitions from inclines to flat running surfaces. These occur in the context of specific recurring trajectories through different environmental

locations, permitting an assessment of how action, trajectory, and environmental location operate in combination to alter spatial tuning in HPC and PPC.

2.2 Methods

2.2.1 Subjects

Adult male Sprague Dawley rats (Harlan Laboratories) were used as subjects (n = 5). Animals were approximately 6 to 12 months of age and individually housed in standard plastic cages. The vivarium was kept on a 12-hour light-dark cycle. To ensure animals were motivated to perform the task, all animals were food restricted to maintain their weight at 85-95% of their original free-feeding weight. Experimental protocols followed all AALAC guidelines and were approved by the Institutional Animal Care and Use Committee guidelines at the University of California, San Diego.

2.2.2 Apparatus

A 1.65 meter squared spiral track with five loops that allowed for movement in both horizontal and vertical dimensions was used (see figure 1a). The four outer loops each had a series of stairs on segment 1 and a ramp on segment 2 while segments 3 and 4 were flat. The outermost loop had eight steps on side 1, loop 2 had six steps, loop 3 had four steps, and loop 4 had two steps. The innermost loop was flat on all sides. The track edges were 1.27cm tall to allow the animal to clearly see distal cues on the walls of the 304cm x 457cm environment.

2.2.3 Behavioral Training

Animals were trained to traverse inbound and outbound along the track, completing each loop of the spiral and receiving a food reward upon completing an inbound run at the center of the spiral, and upon completing an outbound run. Animals

were trained to run ballistically without pausing in order to get a clean analysis of spiking data as it relates to traversing the track.

2.2.4 Surgery

Once rats were trained, Isoflurane (4-5% induction, 1-2% maintenance) was used to anesthetize animals for surgery, and they were placed in a stereotaxic apparatus (Kopf Instruments). After craniotomy and resection of dura mater over the left and right PPC (anterior-posterior: 4mm posterior to bregma, 2.3mm lateral to the midline suture, 0.5mm depth from brain surface), rats were implanted with tetrode arrays (bundles of four 12µm tungsten wires, gold plated to impedances of 0.1 mOhms) mounted to custom-fabricated microdrives that allowed wires to be moved ventrally through PPC across days in 40µm increments until reaching the hippocampus. Tetrode locations within CA1 were verified by the presence of sharp-wave ripple events in vivo, and then later confirmed in the histology by the presence of wire tracks in CA1. All surgeries were performed in compliance with the Institutional Animal Care and Use Committee guidelines at the University of California, San Diego.

2.2.5 Recordings

The recording techniques utilized for the current study have been described in detail in prior publications from the Nitz Laboratory (Alexander & Nitz, 2015; Nitz, 2012). Recordings of both PPC and CA1 multiple single neuron populations and local field potentials were obtained during track traversal. Data was collected with a 48-channel Plexon system that coordinates signal amplification, filtering, and sampling of waveforms. Action potentials were amplified at the headstage connection (20X, Triangle Biosystems), the pre-amp stage (50X), and at the amplifier stage (1-15X). A bandpass

filter (450Hz-8.8Hz) was applied and spike waveforms were digitized using SortClient (Plexon, 40kHz sampling).

Two overhead and one side camera recorded the animal's position on the track in all three dimensions (figure 1b) using Cineplex3D software (Plexon, Inc., Denison, TX). Cineplex 3D detects differently-colored LED lights attached to the rat's implant and encodes head position and orientation in all three dimensions. Such tracking affords identification of direction of movement, head orientation, and velocity in all three dimensions, as well as left and right turning and stair hopping actions. Tracking data was filtered to identify clean, ballistic runs. Only inbound trajectories were used to analyze firing patterns, as outbound runs were far less ballistic.

Each rat had 3 microdrives with four tetrodes each allowing utilization of all 48 channels on the Plexon system. Microdrives were custom-built to allow dorsal to ventral (PPC to HPC) movement of the tetrodes across days, allowing recordings of many neurons from each animal. An approach to CA1 is routinely recognized by the presence of sharp wave ripple events in the local field potential during moments when the animal is idle.

The number of recording sessions in total varied across rats. Analyses include data from the following numbers of recordings from each of the five rats: 26, 40, 17, 21, and 18. Recording sessions typically lasted about 45 minutes each, and on average between 10 and 25 inbound and outbound laps were typically run during each session. Recording sessions where rats ran fewer than 6 laps with uninterrupted locomotion were not used for data analysis.

2.2.6 Histology

After recordings were completed, animals were anesthetized and perfused with 4% paraformaldehyde. Brains were then extracted and sliced into 50μm sections. Nissl stain confirmed wire locations and final wire depth in PPC and CA1 (see figure 1c). Histological records, in particular the final depths of tetrode bundles, were cross-referenced to logs of turning depth for each tetrode bundle and to records noting the first day in which theta-frequency (8 Hz) activity was found in recorded neurons (a feature of most hippocampal neurons) and the first day that obvious sharp-wave/ripple events were observed (indicating close proximity to the CA1 pyramidal cell layer).

2.2.7 Identification of Clean, Ballistic, Track Traversals

A custom-built MATLAB graphical user interface was used to mark trial starts and ends from the tracking data to identify individual clean, ballistic trials. Trials were manually categorized into inbound and outbound trajectories, and only clean ballistic runs (i.e., having uninterrupted locomotion) were used in analyses of neural activity in order to prevent confounds such as pausing and consuming food rewards between trials, and so that every location is reliably associated with the same action and head orientation. PPC is sometimes sensitive to action, and HPC patterns can change as rats exhibit exploratory head-scanning behaviors (Monaco, Rao, Roth, & Knierim, 2014). Trials that were dropped from analysis included trials where the animal paused its run for any reason. Only inbound trajectories were used to analyze firing patterns, as outbound runs often did not meet criteria for clean, ballistic traversals. Positional rate vectors for each neuron were constructed by mapping the animal's location to a track template having 905 evenly-spaced spatial bins (2.24 cm in length).

2.2.8 Linearized Firing Rate Calculation

Linear firing rate vectors for inbound and outbound runs were constructed by dividing the total number of spikes in each template bin (2.24cm) during each trial by the total occupancy time in that bin. These vectors were then averaged across trials to obtain mean cross-trial positional firing rate vectors (see fig 1d,e), which allowed characterization of firing rate activity during track traversals in the form of spatial firing fields or action correlates where neural activity reliably increases.

2.2.9 Unit Isolation

Units were isolated using Plexon's Offline Sorter software. Main clusters were first cut by plotting peak minus valley values of the waveform for each spike from the different tetrode wires on the X and Y axes, and then selecting spikes that form clusters. Then noise was reduced by plotting various waveform features of each spike, such as energy, nonlinear energy, and principal component projections. Spikes that deviated from the main cluster were trimmed away.

2.2.10 Filtering Out Interneurons

HPC interneurons were filtered out of the dataset and were not included in analyses. Interneurons were identified by first locating all bins where the firing rate was below 0.3Hz for each HPC neuron. If a neuron had fewer than ten bins (of 905) with firing rates below 0.3Hz, it was considered an interneuron and dropped from the dataset.

2.2.11 Correlation Matrix Construction

To examine activity patterns for the entire population of neurons and compare this activity at different track locations (across loops, segments), correlation matrices were created (see figure 2a-b). As reported in other publications (Alexander & Nitz, 2015; Cowen & Nitz, 2014; Maurer, VanRhoads, Sutherland, Lipa, & McNaughton, 2005), the

matrices allow for assessment of similarity in spatial mapping across different track locations. To this end, firing rates of all neurons at a particular position bin was correlated with the firing rates of all neurons at every other position bin. Correlations for all possible track bin comparisons were collected and put into a matrix. These allowed for examination of similarities in firing patterns at different bin positions, across the entire population of PPC or HPC neurons.

2.3 Results

2.3.1 Tuning of Posterior Parietal Cortex and Hippocampal Neurons to Track Locations with Specific Actions

Adult male rats (N=5) were trained to run inbound and outbound trajectories in an uninterrupted fashion along a squared spiral track with five loops (figure 1a, 1b). Two-hundred eighty PPC and 170 HPC neurons were recorded and included in analyses. While our implantation target lies within PPC, we note that PPC is narrow along the anterior-posterior axis and that it is possible that some PPC neurons might better be regarded as V2. Overall mean firing rate for HPC and PPC was 1.18Hz and 6.56Hz, respectively. Firing patterns for deep-layer PPC and HPC-CA1 neurons (figure 1c) were analyzed for inbound trajectories only, as these had very smooth, ballistic running behavior compared to outbound trials. Where most mazes utilized in studies of spatial mapping demand only left and right turns and straight running along flat surfaces, movement through this maze expands beyond this typical range of behaviors to include stair hopping (segment 1 for each of outer four loops; figure 1a, colored lines), moving up and down an incline (segment 2 of the outer four loops), and managing transition

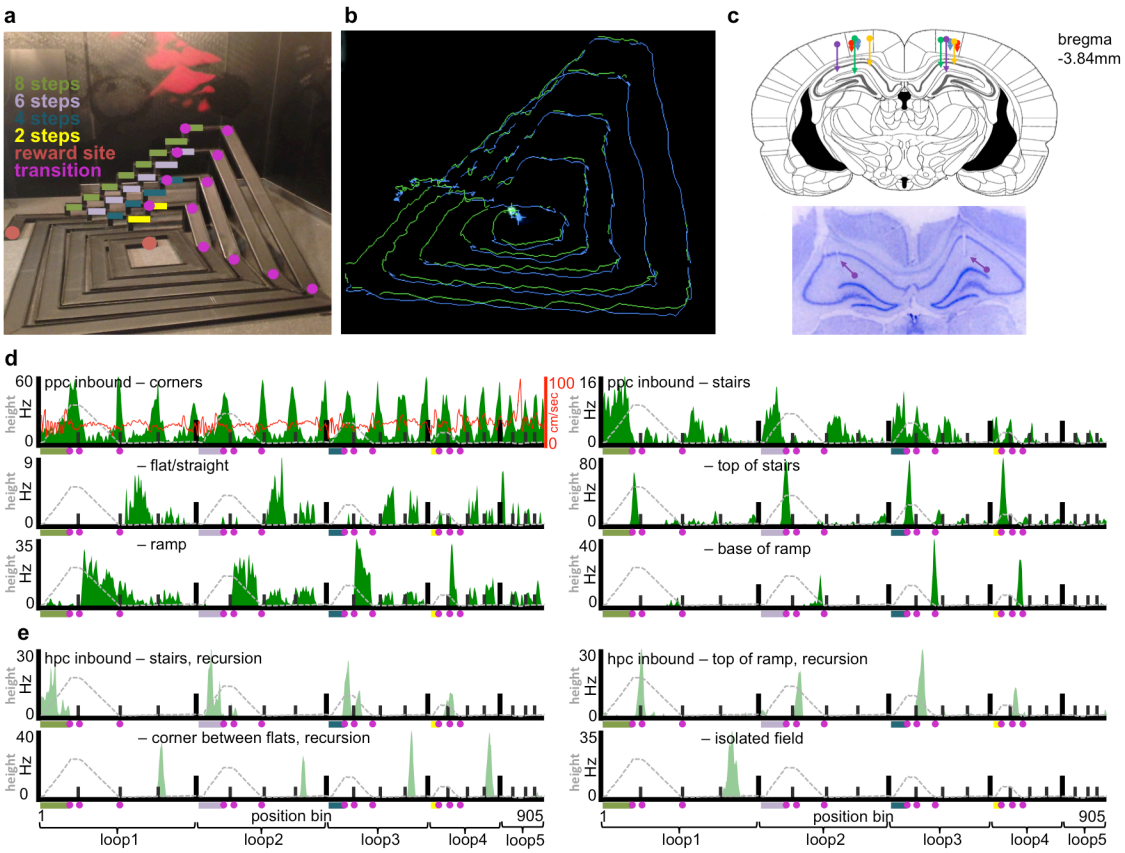

Figure 1. The squared spiral track and associated firing rate vectors for PPC and HPC neurons. (a) Photograph of the three-dimensional, squared spiral track in the recording room with stairs highlighted by colored lines. The outer loop 1 has 8 steps (green), loop 2 has 6 steps (lavender), loop 3 has 4 steps (blue), loop 4 has 2 steps (yellow), and loop 5 is flat. Transition zones (purple circles) and reward sites (red circles) are also indicated. **(b)** Three-dimensional tracking data for one example trial. Blue and green traces show tracking for each light (blue and green LEDs) attached to the animal's implant. **(c)** Electrode placements for all animals. The reconstructed tetrode bundle trajectories are depicted for each of the five animals used in the study with the left and right bundle trajectories for each animal indicated by different colors. Example histological section for one animal with arrows marking the final depth of tetrode bundles. **(d)** Example PPC firing rate vectors for inbound runs. Shown are action correlates mapping corners (upper left), flats (middle left), ramps (bottom left), stairs (upper right), top of stairs (middle right), and base of ramps (bottom right). Gray dashed line depicts animal height (max = 90cm). Red trace in upper-left example rate vector corresponds to movement velocity in cm/sec (velocity axis given on right side of plot). Loops are demarcated by bolder, taller black lines, and segments are demarcated by thinner, shorter black lines. Color coding for steps and transition zones used in figure 1a is also depicted along the x-axis here. **(e)** Example inbound HPC firing rate vectors showing recursion on analogous parts of the track (upper and lower left, upper right) and an example of an isolated field (lower right). Loops are demarcated on bottom by brackets.

points between ramp and flat sections. For added contrast, the innermost loop is flat on all four segments.

We first established that actions related to movement in the vertical dimension could impact the firing activity of PPC cells. In addition to turning related activity and activity specific to flat running sections in the horizontal dimensions (figure 1d, upper left and left middle), firing rate vectors of individual neurons also exhibited activity constrained to the locations associated with specific vertical moving actions. These include recurring activity that was modulated according to location in the full route over stair sections (figure 1d, upper right), ramp sections (figure 1d, bottom left), and transition points between stairs to flat areas and ramps to flat areas (figure 1d, right middle and right bottom right). Finding such action correlates replicates horizontal action mapping found previously on a squared spiral track (Nitz, 2012) and extends it to the behaviors associated with movement through the vertical dimension.

As expected, HPC cells exhibited place-specific firing, but with sensitivity to the recursion of path shape and required locomotor actions inherent in the maze structure. Consistent with prior work, the spatial information (per spike) metric for spatially-specific activity was high in our population of CA1 neurons (mean 3.28 +/- 1.98, median 2.85) relative to PPC (mean 1.07 +/- 1.45, median 0.65). Figure 1e depicts the linearized firing rates of example HPC neurons with place-specific activity isolated to single locations (figure 1e, bottom right) or recurrence of spatially specific firing patterns at analogous locations of each loop. Neurons with recurrence included some that fired over vertical transition points such as the beginning of the downward-going ramp on inbound traversals (figure 1e, upper right).

To approximate the number of HPC neurons that show recursive firing across analogous locations of at least two loops, we first determined the location (loop and segment type) of peak firing for the neuron. If the main peak occurred over stair, ramp, or flat segments of loops 1-4, we then examined whether that neuron also fired at a rate of least 50% of that main peak on analogous segments of one or more of the other loops. Thirty-seven percent of HPC neurons met this criterion. We then calculated this using 25% of main peak firing as a threshold, and 46% of HPC neurons met this more liberal criterion. These numbers are summarized in Table 1.

Table 1. Percentages of HPC and PPC neurons showing recursion in firing across analogous segments of multiple loops at two threshold levels: 50% and 25% of main peak firing.

Recursion	**50% main peak**	**25% main peak**
HPC	37%	46%
PPC	80%	88%

To approximate the number of PPC neurons that show recursion, we used the same criteria as outlined for HPC (Table 1). To further examine PPC action correlates, of the PPC neurons that showed recursion at the 50% threshold, we calculated the percentage of those that had their main peak over a particular segment type (stair, ramp, flat1, flat2), and these numbers are summarized in Table 2. Recursion was relatively evenly distributed across the types of maze segments and the locomotor actions associated with them.

Table 2. Percentages of PPC neurons with peak firing at maze locations sorted by their accompanying actions.

Action correlates - PPC	Main peak
Stair	29.3%
Ramp	25%
Flat1	12.5%
Flat2	13.6%
Corners	44.3%
Top of stairs	10.7%
Base of ramp	7.5%
Top of ramp	6.1%

Of the PPC neurons that show recursion, we wanted to know how many had their main peak in particular areas such as corners or transition areas between horizontal-only and horizontal plus vertical locomotion. We examined the dataset for neurons that met the 50% threshold for recursion and had their main peaks within a window of one of these particular areas. For corners, the range was defined as between the last 25% of any segment, and the first 25% of the following segment. For the top of the stairs and the base of ramps, we looked for recurring neurons with a main peak within 40 cm surrounding the top of the stairs and the base of the ramp on any loop. For the top of the ramp, since it was very close to the corner we used an offset range so as to not overlap with the height of the animal's turn and any portion of the prior segment. The top of the ramp was 10.16cm from the corner. We defined our top of ramp as a 40 cm window that began approximately 7 cm behind the top of the ramp, and extended 33 cm forward from the top

of the ramp on any loop. The main peaks for PPC neurons showing recurrence at the 50% threshold were distributed uniformly across maze locations and the locomotor actions associated with them (Table 2). We note that the sum of Table 2 percentages exceeds 100, as locations such as top of stairs overlap with the stair segment.

2.3.2 Discrimination and Recursion in Posterior Parietal Cortex and Hippocampal Population Firing Patterns

We next quantified the extent to which PPC and HPC population firing patterns discriminated or generalized (recurred) across sub-fields of inbound track traversals. Sub-fields include 'loops', the five squared trajectories making up the entire inbound or outbound routes, and 'segments', the four sections making up each loop. Population correlation matrices were constructed based on the mean firing rates for each neuron on odd-numbered vs even-numbered track traversals (figure 2a, 2b). As reported in other publications (Alexander & Nitz, 2015; Cowen & Nitz, 2014; Maurer et al., 2005), these matrices allow for a wide-range of assessments of similarity in spatially specific tuning across PPC and HPC populations across different track locations and to examine reliability in tuning at any single location. To construct these matrices, we determine the Pearson correlation between the set of firing rates across all neurons for all pairwise track locations. The use of mean rate vectors from odd versus even numbered track traversals permits assessment of reliability in spatial tuning for any single location. Correlation values for all possible track location comparisons are entered into the matrix, the axes for which are organized by location on the track. Matrix values along the main diagonal of the matrix (moving from upper left to lower right) reflect reliability in population patterning for the same location on different trials (figure 2c, black trace).

Figure 2. Quantifying recursion in population firing patterns between track locations. (a-b) Correlation matrices for PPC and HPC population firing patterns on inbound runs. Segments and loops are demarcated by thin and thick black lines, respectively. The full traversal corresponds to movement through 905 evenly spaced position bins. **(c)** Schematic depicting portions of the correlation matrix used to compare overlap in population activity patterns across loops (upper panel) and across segments (lower panel). The lower panel is a magnified version of the upper left square in the upper panel. Specific comparisons are color-coded to match color code for traces in d,f, and h-k. Purple shading highlights location of loop 1 correlation values. S, R, F1, and F2 denote locations of the matrix associated with, respectively, stair climbing sections, ramp descent sections, and the two flat-run sections. **(d,f)** Cumulative distributions of PPC and HPC correlations comparing analogous position bins for adjacent loop comparisons and for the main diagonal. The main diagonal values reflect comparison of odd versus even trial mean population firing patterns for the same locations. Each loop comparison (loop 1v2, 2v3, etc.) is represented by a different color, as indicated. Vertical gray line represents correlation threshold of 0.5 (used in e and g) and colored dashed lines highlight where each trace crosses 0.5. **(e,g)** Bar charts showing proportion of correlations under 0.5 for each loop comparison for PPC and HPC. Bars are organized according to the degree of spatial separation between loops being compared (1 degree of separation, 2 degrees of separation, etc., indicated by top brackets). Red dashed lines demarcate proportion of correlations under 0.5 expected by chance for these comparisons. Chance levels were drawn from the 95^{th} percentile of correlation matrices constructed from the dataset with firing rate vectors circularly shifted by randomized amounts for each neuron. **(h-k)** Cumulative distributions of PPC and HPC correlations comparing analogous position bins for all segment comparisons and main diagonal within loop 1 (h,j) and loop 5 (i,k). Each segment comparison (stair vs ramp, stair vs flat 1, etc.) is represented by a different color, as indicated. Vertical gray line represents correlation of 0.5, and colored dashed lines highlight where each trace crosses 0.5. **(l)** Bar charts showing proportion of correlations under 0.5 for each segment comparison and main diagonal within each loop for PPC (upper) and HPC (lower). Red dashed lines demarcate the proportion of correlations under 0.5 expected by chance for these comparisons, taken from the 95^{th} percentile of correlation matrices constructed from the dataset with the firing rate vectors circularly shifted by randomized amounts.

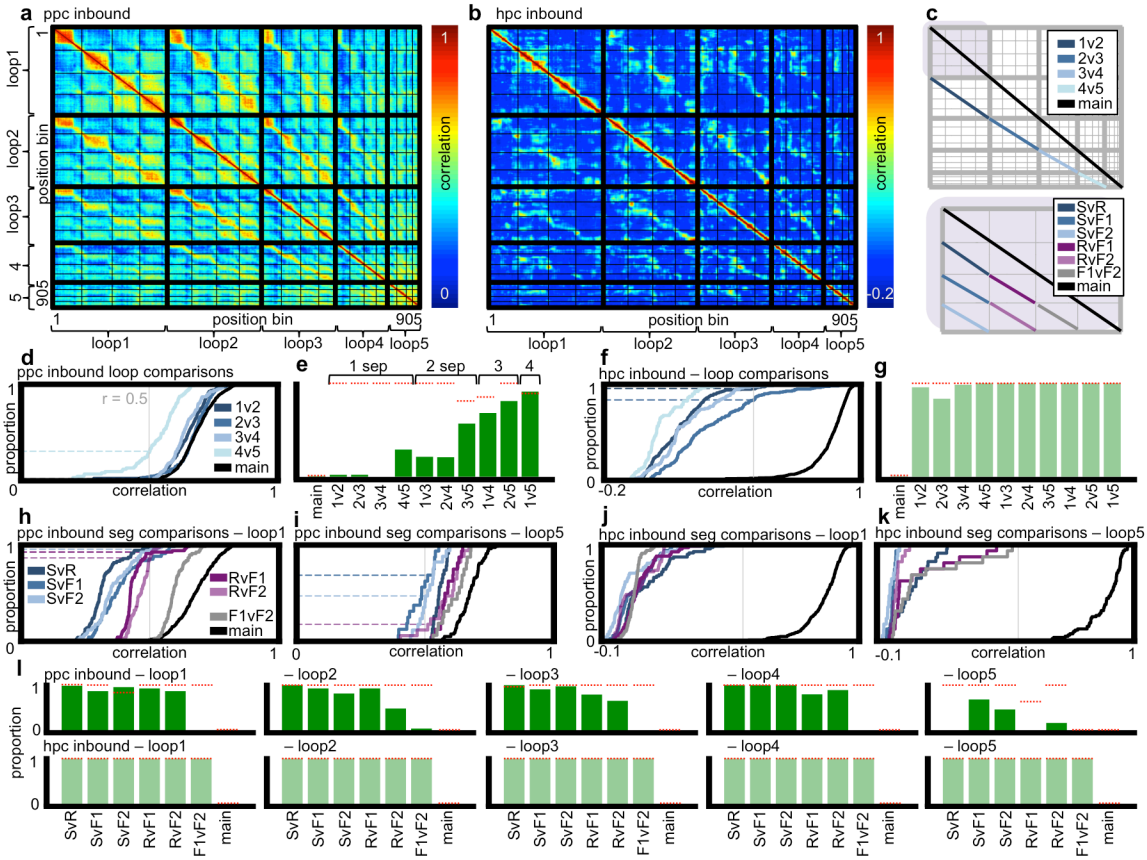
a
ppc inbound
loop1
loop2
loop3
4
5
position bin
1
905
correlation
1
0
loop1
loop2
loop3
loop4
loop5
b
hpc inbound
-0.2
c
1v2
2v3
3v4
4v5
main
SvR
SvF1
SvF2
RvF1
RvF2
F1vF2
d
ppc inbound loop comparisons
r = 0.5
proportion
e
1 sep
2 sep
3
4
main
1v2
2v3
3v4
4v5
1v3
2v4
3v5
1v4
2v5
1v5
f
hpc inbound – loop comparisons
-0.2
g
h
ppc inbound seg comparisons – loop1
i
ppc inbound seg comparisons – loop5
j
hpc inbound seg comparisons – loop1
-0.1
k
hpc inbound seg comparisons – loop5
l
ppc inbound – loop1
– loop2
– loop3
– loop4
– loop5
hpc inbound – loop1
– loop2
– loop3
– loop4
– loop5

We first examined population correlation values that represented specific combinations of segment and loop sub-fields of the full track (figure 2d-2l). We measured pattern similarity across loops by comparing values from the main diagonal and values from "off" diagonals that represent adjacent loop comparisons of analogous loop positions (e.g., loop 1 vs 2, loop 2 vs 3, etc.; figure 2c, upper). We used a series of Wilcoxon rank-sum tests to statistically compare all cumulative distributions representing each loop comparison. Cumulative distributions for loop versus loop pattern similarity in both PPC and HPC revealed that the main diagonal (figure 2d, f, black traces), representing similarity in patterning for the same loop on odd versus even trials, contained correlation values that were significantly higher than diagonals comparing analogous positions along loops, with the exception of loop 2 vs 3 in PPC (PPC p-values for the values along the main diagonal versus values along diagonals comparing analogous positions along loops to each other ranged from $p = 1.65e\text{-}37$ to $p = 0.08$; the same comparisons for HPC ranged from $p = 1.36e\text{-}122$ to $p = 2.81e\text{-}49$; Bonferroni adjusted alpha = 0.0071). This simply indicates that, despite loop to loop identity in actions taken and directions traveled, the populations of neurons in both HPC and PPC maintained the strongest trial-to-trial reliability in encoding of the same locations along the track.

Similarity in population firing patterns for PPC across loops was quite high for adjacent loops (figure 2d). Thus, for PPC, the same-shaped trajectories and action sequences across each loop yield recursion in population patterning. An exception to this was the relatively lower similarity in PPC population patterns for loop 4 vs 5 (figure 2d,

lightest blue trace; Wilcoxon rank-sum test p-values for loop 4 versus loop 5 correlations versus all other combinations of adjacent loops ranged from p = 1.76e-26 to p = 8.15e-17; Bonferroni adjusted alpha = 0.0071). We note that there are no stairs or ramp along loop 5, and therefore attribute this exception in similarity between adjacent loops as reflecting differences in the associated action sequences.

To extend our examination of PPC loop comparisons, we calculated the proportion of values in each distribution that had a correlation of less than 0.5 for all loop comparisons. When these proportions are graphed according to the degree of separation between any two loops, a clear pattern emerges wherein degree of separation yields greater and greater PPC population pattern dissimilarity (figure 2e). Additionally, we calculated the proportion of correlation values below 0.5 for each loop comparison that would be expected by chance by reconstructing correlation matrices from circularly shifted firing rate vectors. Each neuron's firing rate vector was circularly shifted (relative to start and end) by randomized amounts that were at least one segment in length (161 cm). We note that the independence of random shifts across neurons destroys the population activity patterns but retains the structure of firing fields for each neuron. This randomization was done 100 times and a correlation matrix was constructed for each one. Randomized correlation matrices were sorted according to mean correlation and the 95th percentile correlation matrix was used to calculate the proportion of correlation values under 0.5 that we would expect by chance. These values are plotted as red dashed lines in figure 2e. Actual proportions below 0.5 only approach chance levels as the spatial separation between loops being compared grows larger. Collectively, these results demonstrate that recurrence in activity is generally high for loops that share a common

set of heading directions and action sequences, but also indicates that progress through the full five-loop route has a strong influence on pattern recurrence as well.

Examining the recurrence in HPC patterns across loops reveals a quite different pattern, one in which recurrence is minimal. Despite strong odd versus even trial reliability in HPC population patterns for the same location, comparison of population patterns between even adjacent loops yields cumulative density functions dominated by low correlation values (figure 2f). While there are correlations slightly above 0 for HPC for loop comparisons, most of these correlations fall well below 0.5 (figure 2g), a threshold that has been used previously to define pattern discrimination across locations for HPC populations (Maurer et al., 2005). The proportions of correlations below 0.5 for each loop comparison are at or near chance levels indicated by red dashed lines (figure 2g). Some recursion was demonstrated in the firing patterns of individual neurons (Figure 1e), but these cases proved infrequent enough that pattern recursion at the level of full neuron population is not robustly observed. As for PPC, HPC correlations for loop 4 vs 5 are the lowest (figure 2f, lightest blue trace; p-values for correlations for analogous positions along loop 4 versus loop 5 versus the same for all other adjacent loop combinations ranged from $p = 3.64e\text{-}21$ to $p = 2.59e\text{-}7$ according to Wilcoxon rank-sum tests; Bonferroni adjusted alpha = 0.0071). This indicates that the presence of movement in the vertical plane can significantly impact population activity patterns in HPC, negating even low-level recurrence to patterns across analogous and adjacent locations in the horizontal plane.

Next we looked at the segment comparisons within a loop, which allowed more direct examination of the influence of the type of locomotor action (figure 2h-l; see figure

2c, lower panel, for schematic of correlation matrix diagonals representing the different segment comparisons). Loops 1-4 each had one segment that required traversing stairs, one segment that required descending ramp running, and two flat running sections. Given the type of action required to traverse each one, action mapping for stair hopping should be rather distinct from both ramps and flats. As far as actions required, we consider ramps to be more similar to flats in that ramps and flats both are associated with alternating movements of the left and right limbs. Stair climbing involves a "hopping" motion in which the left and right limbs move in parallel. Additionally, based solely on a model in which action drives activity patterns, the two flat segments should be mapped very similarly to each other. We used a series of Wilcoxon rank-sum tests to statistically compare all cumulative distributions representing each segment comparison within a loop (e.g., stairs vs ramp of loop 1 compared to stairs vs flat 1 of loop 1).

In PPC, similarity in type of locomotor action was a strong determinant of population pattern recurrence. Within loop 1, main diagonal correlations representing the same positions along each segment for odd vs even trials (figure 2h, black trace) were significantly higher than any segment-segment comparisons (p-values ranged from $p = 1.15e-38$ to $p = 7.99e-15$; Bonferroni adjusted alpha = 0.0033). Correlations between analogous positions along the two flat segments (figure 2h, gray trace) were significantly higher than all other segment-segment comparisons (p-values ranged from $p = 3.23e-24$ to $p = 4.31e-19$; Bonferroni adjusted alpha = 0.0033). The correlation values for the stair and ramp segment (figure 2h, darkest blue trace) were significantly lower than all other segment comparisons (p-values ranged from $p = 3.23e-24$ to $p = 4.52e-4$; Bonferroni adjusted alpha = 0.0033). Position bin comparisons among flat segments (figure 2h, gray

trace) had the highest correlations (figure 2h, gray trace; figure 2a correlation values for flat comparisons, can be seen more clearly in figure 3a). The bar graphs of figure 2l (top row) show the proportion of correlations below the 0.5 threshold for the PPC population. From this perspective, the population patterns for flat sections versus ramp sections are quite different. Flat comparisons (F1 vs F2) have the lowest proportion (near zero) in every loop. Finally, across loop 5, where all four segments are flat, each segment-segment correlation distribution exhibits many high values (figure 2i) and few values below 0.5 are observed (figure 2l). Flat sections in loops 1-4 were mapped more similarly to each other, and all segments of loop 5 were mapped more similarly, due to their similarity in actions (flat running, left and right turning behavior).

As expected (Nitz, 2011), HPC populations completely discriminated all segments, no matter their required type of locomotor action as illustrated by overall lower correlation values among segment comparisons (figure 2j-l). Correlations representing the main diagonal on odd vs even trials for loop 1 (figure 2j, black trace) were significantly higher than all segment-segment comparisons according to a series of Wilcoxon rank-sum tests (p-values ranged from $p = 8.77e-39$ to $p = 1.61e-37$; Bonferroni adjusted alpha = 0.0033). Additionally, loop 5 segments did not appear any more or less correlated than segment comparisons from other loops (figure 2k, l bottom row), and main diagonal correlation values (figure 2k, black trace) were significantly higher than all segment-segment comparisons (p-values ranged from $p = 3.57e-13$ to $p = 1.19e-10$; Bonferroni adjusted alpha = 0.0033). Thus, HPC exhibited strong reliability across trials for the same locations, but similarity in locomotor action did not drive extensive similarity in mapping at different locations.

2.3.3 Posterior Parietal Cortex and Hippocampus Scale of Representation Follows Variation in Type of Locomotor Action

The scale at which the population of HPC neurons is spatially selective has been previously defined by the distance at which the correlation falls below 0.5 (Maurer et al., 2005). Some reports indicate that the scale of representation is stable for any single location within the CA1 region, but that scale varies along the longitudinal (dorsal-to-ventral or septo-temporal) axis of HPC and medial entorhinal cortex (Kjelstrup et al., 2008; Hafting et al., 2005). Others report that the scale might be more dynamic, based on running speed, path length, and position relative to inflection points in behavior (e.g., turns and reward consumption sites, Gupta, van der Meer, Touretzky, & Redish, 2012). By measuring, for all locations, the distance from any point associated with a drop in population correlation below 0.5, we sought to reveal other factors that modulate the scale of representation in HPC and PPC.

Depending on the structure of the trajectory, variation between locomotor actions and movement through space are dissociated. This is true of both the spiral track from the current study, and of episodes such as a walk through a city. In our case, the animal traverses long distances up and down ramps, stairs, and along flat surfaces, all covering a great amount of space. The animal crosses much less space when turning and when transitioning from a stair or ramp to a flat surface. Thus, within any episode associated with a traversal along a path, the rate of variation in location can be wildly dissociated from the rate of variation in locomotor actions. We therefore asked how this specific difference is manifest in the scale of spatial tuning in HPC and PPC.

Using the metric for scale of representation indicated by Maurer and colleagues (Maurer et al., 2005), we took the correlation matrix main diagonal and found the distance (perpendicular to the main diagonal) at which correlations dropped below a threshold of 0.5 (similar results were obtained using thresholds between 0.25 and 0.65). Dropoff points are plotted in black over loop 1 correlation matrices, thereby depicting dynamics in the scale of representation in PPC and HPC for loop 1 (figure 3a-b). These distances are plotted in green (PPC) and black (HPC) green in figure 3c, and the difference between the two (PPC minus HPC) is plotted in blue, graphically illustrating the scale of representation for different positions along the entire track.

Both PPC and HPC exhibit a fluid dynamic in spatial scale that follows the variation in type of locomotor action (figure 3c). In PPC, the scale appears to more closely follow the actions, in that variation in loop 1 is greater than loop 2, variation in loop 2 is greater than loop 3, etc. HPC shows the same dynamic, however it is in a compressed form. To quantify these changes, we determined the mean values for scale of representation for the middle half of each track segment and compared them to means for the remaining 50% of space that surround each turn (as indicated by pink and blue shading along loop 1 in figure 3c). Figure 3d depicts these values for all segments as well as the mean values for each loop (mean values are connected by lines, color coded for loop as indicated). With the exception of loop 5 data, centers of segments were associated with greater spatial scale of representation than for corners in PPC (figure 3d, leftmost panel). A Wilcoxon rank-sum test revealed an overall significant difference between centers of segments and corners for all loops for PPC ($p = .006$). Perhaps owing to the very short spaces between loop 5 turns, and perhaps due to the fact that there is no

vertical component in loop 5, the scale of representation in PPC sharply rises over the middle of the loop. In HPC, a similar reduction in scale of representation around turns is observed, but the overall effect is dampened and did not reach significance when all loops were considered ($p = .34$; figure 3d, middle panel). Nevertheless, the PPC and HPC vectors for scale of representation across the entire track are significantly positively correlated ($r = 0.36$, $p = 1.89e\text{-}29$) and the comparison of segment centers versus corners for HPC is significant for values taken from loops 1 and 2 ($p = .015$). Figure 3d (rightmost panel) depicts these values separately for PPC and HPC to allow comparison between the two brain regions. A Wilcoxon rank-sum test demonstrates significant differences between PPC and HPC in scale of representation for both centers of segments ($p = .00007$) and corner comparisons ($p = .002$). This suggests a constraint on the range of dynamics in scale of representation for HPC relative to PPC.

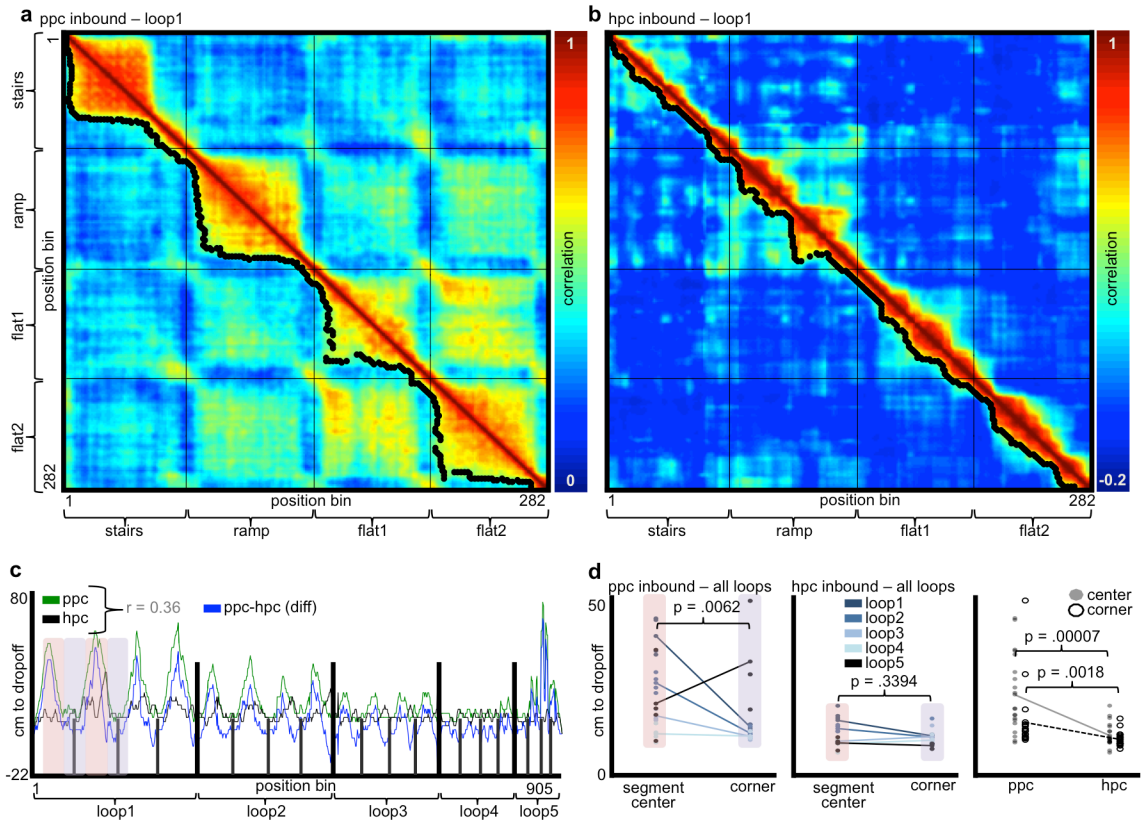

Figure 3. PPC scale of mapping reflects the segment and loop structure of the entire track. (a-b) Loop 1 inbound population correlation matrices for PPC and HPC, respectively. Perpendicular distance from diagonal where correlation first drops below 0.5 is plotted in black. **(c)** Perpendicular distance from diagonal plotted for entire track. PPC plotted in green, HPC plotted in black, PPC-HPC difference trace plotted in blue. Pearson correlation of r = .36 between the PPC and HPC traces is indicated. Loop transitions are marked with bolder, taller black lines, segment corners are marked with shorter, thinner black lines. The middle half of each segment (centers) for loop 1 are highlighted in pink. The remaining 50% of space that surrounds each turn is highlighted for loop 1 in blue. **(d)** Mean drop-off distance (distance from diagonal at which population correlation drops below 0.5) at segment centers and corners for HPC and PPC. Mean drop-off distance of center bins for each segment for every loop are plotted as dots on left of each graph while corners are plotted on right of each graph (left and middle panels). Loop means are connected by lines. Pink and blue boxes highlight segment center peaks and corner valleys to match c. Each loop (1-5) is depicted in a different color as indicated. Right panel depicts these values, but visually compares PPC and HPC on centers and on corners in one plot. Centers are plotted in solid gray ovals while corners are plotted in hollow black ovals. Solid and dashed lines connect means.

2.4 Discussion

The spatially-specific firing patterns of HPC have often been used to gain insight into the content of episodic memory as it relates to movement through locations in an environment. In the present work, we extend such considerations to include the PPC, a structure that, in humans, is associated with the perception of spatial relationships in both egocentric and allocentric frames of reference (Pouget & Driver, 2000; Driver & Mattingley, 1998; Crowe, Averbeck, & Chafee, 2010; Benoit & Schacter, 2015; Saj et al., 2014; Hassabis et al., 2007).

Episodic memories are not just memories for places, but memories for the actions taken as one moves through those spaces including turns, long stretches, walking up and down hills, transitioning from a steep hill to a flat surface, and navigating space as the constraints of the environment will allow. Furthermore, memory for the time spent on each action is often disproportionate with the amount of time experienced while performing those actions. Therefore we examined firing patterns for HPC and PPC neurons as a function of location on a five-loop, squared spiral track. Each loop had four segments: a stair segment, a ramp segment, and two flat segments. Segments of the innermost loop were all flat. The track design was implemented to achieve recursion in path shape across each loop and to extend the number of different locomotor actions utilized in path running. Both locomotor action and path recursion have previously proven to powerfully impact the form of spatially-tuned firing in both HPC and PPC, yielding both discrimination for individual locations based on overall trajectory (Ferbinteanu & Shapiro, 2003; Frank et al., 2000; Wood et al., 2000; Ainge et al., 2007; Grieves et al., 2016) and recursion in firing patterns across different locations when

trajectory shapes are repeated (Nitz, 2011; Frank et al., 2000). We consider here the extent to which path shape and locomotor action impact: 1) the generalization or discrimination in population firing patterns for different environmental locations, and 2) the scale of representation in PPC and HPC. We found that PPC population activity patterns, through their discrimination and similarity in firing patterns, mapped location, actions, and progress through a trajectory. Additionally, PPC and HPC's scale of representation followed variation in the type of action performed during track traversal. The results speak to the brain mechanisms which encode path running episodes in a way that goes beyond memory only for locations visited to include the actions taken along trajectories of a particular shape.

Mapping positions in the vertical dimension, by most accounts, is anisotropic (Hayman, et al., 2011; Hayman et al., 2015; Casali et al., 2019) to that for the horizontal dimensions. However, as we have stated, episodic memories associated with trajectories through space are also characterized by the action that takes place. The current study shows that the vertical actions yield specific activations of PPC neurons, and clearly impact the degree to which both PPC and HPC neuron populations produce similar or different activity patterns for equally distant locations. Linearized, positional firing rate vectors of the squared spiral track revealed a number of neurons in PPC whose firing peaks coincided with track positions associated with specific actions such as turning, hopping (along the stair section of loops 1-4), downward motion along a ramp segment, and transitions from movement through vertical and horizontal planes to movement through only the horizontal plane. Accordingly, PPC population firing patterns exhibited similarity across track spaces that followed similarity in actions. From population

correlation matrices measuring similarity in firing patterns between all pairs of track locations, the greatest between-location similarity was seen for path segments that demanded the same actions. Spatial tuning along the track's two flat segments, which required forward locomotion bracketed by right turns and had no vertical components, bore greater similarity to each other than did the flat and ramp segments. Similarity was still further reduced when comparing the two flat segments to the ascending staircase which demanded hopping, a very different form of locomotion. Additionally, all segments in loop 5, which were flat, demanded no vertical movements, and required similar actions, showed greater similarity to each other than did all segments in loops 1-4 which varied in vertical components and actions. Thus, action type was a strong determinant in the mapping by the population of PPC neurons and differentiates actions associated with movements in horizontal versus vertical dimensions.

While the impact of locomotor action on PPC pattern recurrence was impressive and graded according to locomotor similarity, we note that PPC firing patterns exhibited greatest similarity along the main diagonal of the correlation matrix which measures pattern similarity for the same locations on odd versus even trials. We also note that pattern similarity was highest for analogous positions along segments that demanded the same actions when those segments were from adjacent loops along the full five-loop path. Thus, while the PPC population showed strong modulation by action type, the location of the animal along the full five-loop route is also a strong determinant of spatial tuning (see also Nitz, 2012).

While some HPC neurons appeared sensitive to position along the track and current locomotor action type, the impact of locomotor action type alone was subdued,

relative to PPC. Pattern similarity across analogous positions of two different segments for any given loop was uniformly low. Thus, as one might expect, recurrence in locomotor actions across the four segments making up each loop was insufficient to drive similarity in firing patterns given the difference in heading directions (McNaughton et al., 1983) and locations in the environment. While locomotor action type was insufficient to drive HPC pattern similarity across different loop segments or even across analogous locations of adjacent loops, the impact of locomotor action on the scale of representation followed a very similar pattern for PPC and HPC. As in earlier work (Maurer et al., 2005), we measured the scale of representation as the distance from any single location past which the population firing pattern for that location versus another falls below $r = 0.5$. We note that while the choice of $r = 0.5$ is somewhat arbitrary, it appears to match the average sizes of place fields along tracks and effectively described reliable differences in HPC place field sizes along the septo-temporal axis. Furthermore, our own results are robust to a range of thresholds between $r = 0.25$ and $r = 0.65$.

Remarkably, the scale, or resolution, of spatial representation in both PPC and HPC fluidly follows variation in the actions that are used to move through space, providing a potential explanation for the irregularity of time recalled in an episodic memory. For example, if one takes a trip that involves driving down long, straight roads separated by turns, the portions of the drive down long straight roads last much longer than the turns. However, the act of turning is an inflection point in the experience, and leaves a stronger impression on the memory for the trip. Thus, the remembered experience of time is highly irregular, perhaps in part as a consequence of the connection of locations and the actions associated with them. The PPC population exhibited a greater

range in scale, exhibiting long stretches of similar activity patterns across segment spaces associated with the same locomotor behavior, be that hopping, descending along a ramp, or simply forward locomotion. Such stretches of sustained PPC firing patterns were interrupted as animals moved through turns, where the scale of representation was minimal. PPC dynamics in scale of representation weakened as the animal moved through inner loops such as loop 4 where the distances associated with forward locomotion along a segment were shorter relative to the spaces over which a full turn is accomplished. Scale of representation in PPC again peaked along the fifth loop, across which the animal's behavior consisted of continuous straight running on a flat surface and right turning for all segments, without vertical traversal.

We found that HPC spatial tuning was highly dynamic in terms of scale and that its patterning follows that of PPC. However, the range of scale was muted relative to PPC. Thus, PPC and HPC, from the perspective of scale of representation, are observed to exhibit parallel sensitivity to the actions that accompany movement through distinct locations in an environment. It is possible, of course, that both structures are influenced in this way by input from another brain region, but the repeatedly observed sensitivity of PPC neurons to locomotor action types and their associated postures (Mimica et al., 2018; Nitz, 2006; McNaughton et al., 1994; Wilber et al., 2014; Whitlock et al., 2012) suggests that HPC sensitivity to locomotor action is a property of interaction between the two regions. PPC and HPC are only indirectly connected through structures such as retrosplenial cortex, peri-rhinal and post-rhinal cortex, and the medial and lateral entorhinal cortex (Burwell, 2000; Witter et al., 2000; Olsen, Ohara, Iijima, & Witter, 2017; Wyss & Van Groen, 1992). Thus, the means by which such parallel dynamics in

scale of representation occurs demand further study. Future work should also address whether the shorter range for scale of representation in HPC is a consequence of local, HPC-centered constraints on persistence in population patterning across space or a compression of the impact of PPC output on HPC through intervening structures.

Both HPC and PPC neurons are strongly implicated not only in spatial mapping, but also episodic memory. As a result, the spatially tuned firing patterns in each region across defined trajectories can be considered a window onto the content and character of episodic memories. From this perspective, the findings from the present work would suggest that memory for the actions taken in series during a path traversal are registered in PPC in a form that also respects the progress through the full route. In episodic memory recall, one would expect that HPC and PPC activity is temporally coordinated to the extent that recalled memory contains the sequence of environmental locations, the sequence of trajectory positions, and the sequence of associated actions. This is at least consistent with the finding that PPC and HPC firing patterns during path traversal are "reactivated" during hippocampal sharp-wave ripple events at stopping points along a trajectory or during subsequent sleep (Qin, McNaughton, Skaggs, & Barnes, 1997).

To the extent that different population patterns reflect distinct elements in episodic memory, we conclude that time in episodic memory is irregular. Population patterns persisting across space do so over several seconds of clock time while the much shorter time periods involved with turning a corner are associated with sharp changes in population patterning. In this way, we expect the action and route location mapping in the PPC population impact the HPC population such that inflection points in behavior

become inflection points in memory with generalization across periods of time that intervene.

Chapter 2, in part, has been published in *Hippocampus,* Shelley, L.E. & Nitz, D.A. (2021). The author of the dissertation is the primary author of this publication.

Chapter 3: Experiment 2 – Choice Behavior and Logical Fragmentation of the Environment

3.1 The Present Study

When asked to judge the location of Montreal relative to Seattle, participants will often state that Montreal is to the northeast, but the actual direction is southeast (Stevens & Coupe, 1978). Similarly, participants will often judge Reno, NV to be northeast of San Diego, CA, when the actual direction is northwest (Stevens & Coupe, 1978). These examples reveal fragmented structure of our cognitive representations of spatial relationships, an idea well-supported by the human spatial navigation literature (Stevens & Coupe, 1978; Hirtle & Jonides, 1985; McNamara, 1986). Spatial locations like San Diego and Reno can be grouped into larger fragments of space like California and Nevada. The relative locations of those larger fragments (e.g. Nevada is east of California), will then sometimes distort judgments of relative direction of subordinate locations (Stevens & Coupe, 1978; Hirtle & Jonides, 1985).

Fragmented environments can also distort subjects' judgments of absolute distance, where distances between landmarks located across fragment boundaries or between clusters tend to be overestimated, and distances within fragments or clusters tend to be underestimated (Kosslyn, Pick, & Fariello, 1974; Hirtle & Jonides, 1985; Newcombe & Liben, 1982; McNamara, 1986). When people plan the shortest route to multiple targets, they opt to use a fragmented, hierarchical navigation strategy that incorporates this phenomenon (Wiener, Ehbauer, Mallot, 2009). Both humans and animals typically must travel long distances all while navigating around barriers and obstacles. Fragmented representations of space may aid animal navigation in much the

same way that knowing the relative locations of every city in the United States is aided by grouping those cities into states and knowing the locations of those states.

One obvious way to break up an environment into fragments is to introduce a barrier. Humans and animals regularly encounter barriers that break up environments into smaller sections. Everyday environments are naturally broken up into smaller sections by physical barriers, but more subtle aspects of an environment may also play roles in logical fragmentation.

A rule can break up visual field space into fragments even when there is no visible, concrete boundary line. For example, one discerns and learns the rules for behavior when on one side versus the other of a speaker's podium. The audience sits in front of the podium and pays attention to the speaker, who makes sure to stand behind the podium and present. In another example of rule-based fragmentation, Freedman and Assad (2006) were able to use a rule to create such a boundary for monkeys. Monkeys were trained to group directions of motion on a screen into two categories, separated by an invisible, but implied category boundary.

The work by Freedman and Assad was focused solely on fragmenting the space on a computer screen with head-fixed animals and so does not speak to the issue of whether an environmental space can be fragmented by a rule in the context of animals traversing through space. Furthermore, space is often mentally organized according to how it is used. Even an essentially wall-less environment will be spatially perceived according to how actions (e.g., cooking) or even lack thereof (e.g., sleeping) are apportioned. Thus, addressing these issues will, in principle, yield important new insights

into how highly complex operations associated with everyday behaviors can yield a fragmented structure in our cognitive representations of the environment.

3.2 Methods

3.2.1 Subjects

Adult male Sprague Dawley rats (Harlan Laboratories) approximately 6 to 12 months of age were used as subjects (n = 8). The rats were housed individually in standard plastic cages and kept on a 12-hour light-dark cycle. Animals were maintained on a food-restricted diet (85-95% of free-feed weight) to motivate them to perform the task. All animals were habituated to the colony room and handled for 30 minutes to 1 hour each day for 1-2 weeks prior to task training. All experimental protocols adhered to AALAC guidelines and were approved by IACUC and the UCSD Animal Care Program.

3.2.2 Apparatus

The behavioral task was conducted using a T-shaped track with a round start-plate (18.5cm diameter) at the base. The track was 122 cm long x 10 cm wide on the stem and 67.5 cm long x 10 cm wide on the top. A 0.5 cm tall railing enclosed all sides, allowing the animal to see the larger room and distal cues on the walls.

3.2.3 Behavioral Training

Animals were trained to traverse the stem of the T-shaped track and make either a left or a right turn at the choice point for a food reward. Correct left or right choices depended on the track's position in the room in relation to an implied, rule-defined boundary (figure 4b). The animals then made a return run, retracing their outbound trajectory directly back to the start plate. Only correct turns on outbound runs were rewarded, and rats received a smaller reward for inbound runs to motivate prompt returns

to the start plate. Animals were trained to run in a ballistic fashion to eliminate pauses that would influence analysis of spiking data. There was no visible, physical line drawn dividing the room. Animals were able to localize themselves by reference to prominent, fixed distal cues in the 304 cm x 457 cm recording room. Track locations were placed 20 cm apart for locations 1-5 and position 6 was located 10 cm adjacent to position 1 (figure 4a). Track location distribution spanned most of the length of the room. Fixed distal cues included large wall murals, a desk, a table, and the recording rig, all distributed around the perimeter of the room.

Initial training involved only track sites 1-4 in larger blocks of 20 trials in each location in randomized order. During a block, the track was placed in one of the 4 locations, and then moved to another location at the start of the next block. Track locations were in randomized order. Rats learned through trial and error that track locations 1 and 2 required left turns and locations 3 and 4 required right turns. After 2 weeks of 20-trial blocks, the task structure was broken up into 28 blocks of 5 trials each and performance accuracy was recorded (figure 4a).

Once rats met criteria on track sites 1-4 (significantly above chance and at least 9 days of behavioral results), track location 5 was introduced as a probe trial, with the exception of one rat that was tested on track location 5 before meeting criteria (figure 4a). This served to rule out simple individual associations between place and a correct action and assess for transfer of the whole-room fragmentation to novel positions. Once animals performed significantly above chance on positions 1-5, track location 6 was introduced as a second probe trial (figure 4a). Novel track locations were immediately incorporated into the 28-block structure.

Figure 4. Paradigm for fragmenting a space into two subspaces. (a) Upper: Overhead view of the track location layout. Full T-track only shown for location 1 in red for figure clarity. The other location markers represent the top of the T. Locations 1-4, shown in color, were the main training and recording locations. Locations 5 and 6, shown in gray, were introduced as novel location probe trials to test for transfer of the task rule to new locations. Gray dashed line through the middle of the space represents the fragment boundary implied by the task rule (no actual line exists). Black panels represent distal cues in the room. Lower: Temporal structure of the task. Each block consisted of 5 trials in a particular location before the track was moved to a new location for the next block of five trials. Each session consisted of 28 blocks. Location order was randomized. **(b)** Overview of task in each track location. Each panel shows overhead view of the rat on the track at one of the 6 locations. Turn direction is indicated by blue and purple dashed arrows and the asterisk represents the reward site. **(c-f)** Behavioral accuracy. **(c)** Boxplots of all rats' percent accuracy on the task across days in each track location 1-4. Boxplots highlighted in red only include data from trial 1 of a block, while other boxplots represent all trials. Animals' performance demonstrated a trend toward lower accuracy in trial 1 and lower accuracy in track locations 2-3. **(d)** Mean percent accuracy of each rat in each trial 1-5. Each colored line corresponds to one rat. Accuracy was significantly worse in trial 1 compared to trial 2. **(e)** Mean percent accuracy of each rat in trial 1 of each track location 1-4. All animals' accuracy was significantly worse on track locations closest to the boundary (2 and 3) compared to locations farthest from the boundary (1 and 4). **(f)** Location 5 and 6 probe trial accuracy. Each colored line represents correct vs incorrect turns for one rat across all trials on day 1 when the novel location (5 or 6) was introduced. Line gaps in the top "correct" area represent incorrect turn choices, and are shown below in the "incorrect" area. Each gray dashed line demarcates a new block of 5 trials. All 8 animals turned correctly in location 5 the first time it was introduced, while 6/8 turned correctly in location 6 the first time it was introduced. Rats that missed location 6 quickly learned the correct turn during that same session.

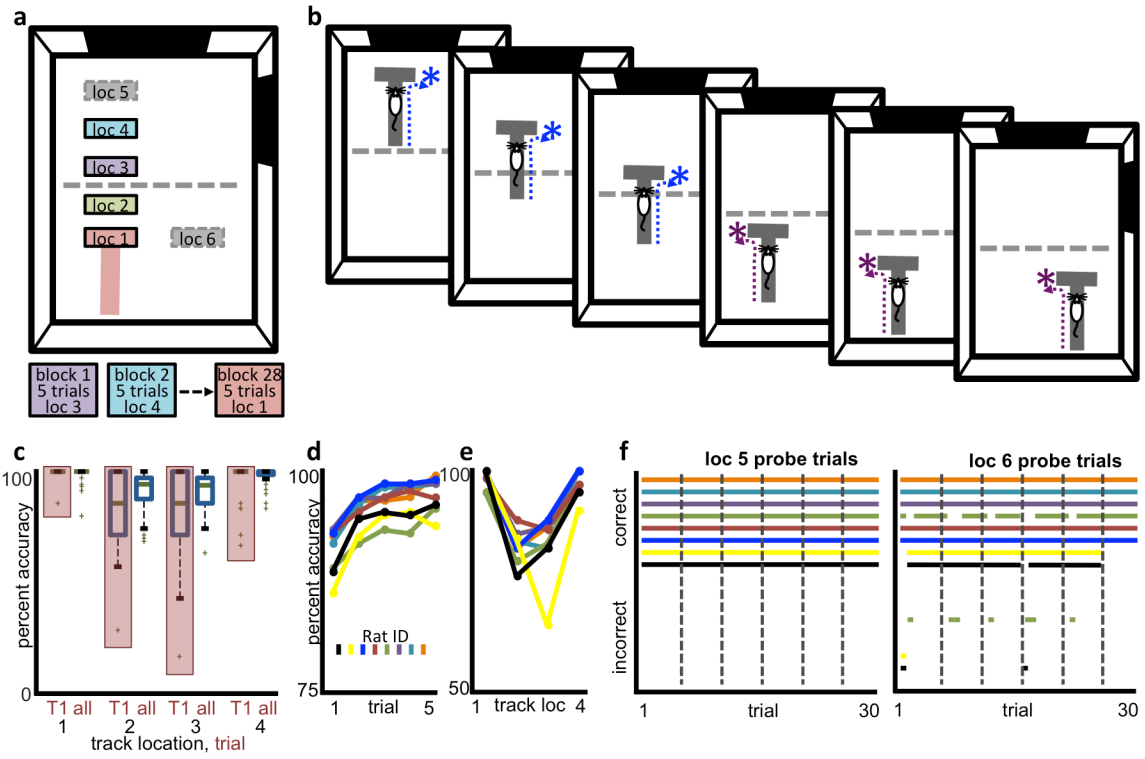
a
loc 5
loc 4
loc 3
loc 2
loc 1
loc 6
block 1
5 trials
loc 3
block 2
5 trials
loc 4
block 28
5 trials
loc 1
b
c
percent accuracy
100
0
T1 all
1
T1 all
2
T1 all
3
T1 all
4
track location, trial
d
percent accuracy
100
75
Rat ID
1
trial
5
e
100
50
1
track loc
4
f
loc 5 probe trials
loc 6 probe trials
correct
incorrect
1
trial
30
1
trial
30

3.2.4 Analysis of Behavioral Accuracy: Trial 1 vs. Other Trials

Sign tests were used to assess whether performance accuracy was significantly above chance (50%) for each trial (1-5) across days before surgery for each of 8 animals and for all animals combined. To statistically assess observed differences in trial 1 vs other trials, a chi square test of independence comparing trial 1 vs trial 2 accuracy was performed.

3.2.5 Analysis of Behavioral Accuracy: Track Location

Accuracy in each track location was evaluated using sign tests to assess whether performance accuracy was significantly above chance (50%) at each track site. For each track location sign test, only data from the first trial of each block was included in this calculation. The first trial of each block is a better assessment of the rat's ability to use knowledge about his allocentric spatial position since the track was moved just prior. During subsequent trials the rat simply has to repeat the action he took in trial 1 if that action was previously rewarded. Sign tests were performed for each location to assess both per-rat accuracy and accuracy of all rats combined. To assess whether rats learned the whole-room fragmentation rule (as opposed to independent place-choice associations), sign tests were also performed on all probe trials (locations 5 and 6) across all rats the very first time the novel location was encountered.

3.3 Results

3.3.1 Choice Behavior Follows the Imposed Logical Fragmentation of the Environment

Adult male rats (N=8) were trained to perform a modified T-maze navigational task in which correct left/right turn choice behavior was dictated by the location of the

maze within the environment (figure 4a). Animals were trained to run along the stem of a T-shaped track and either turn left or right depending on the location of the choice point (intersection) in the larger experimental space. After an outbound run, the animals then made a return run where they ran directly back to the start plate. When the choice point of the maze was in one half of the environment, the animal was required to make a left turn, and if in the other half, a right turn (figure 4b). In order to assess the impact of recent navigational decisions at a single location, animals were run on the task at track locations 1-4 in daily sessions of 28 blocks made up of 5 trials each. Correct decision-making in this task demands learning of a rule-based logical fragmentation of the environment (the 'allocentric space'). By rule, maze locations in one half of the room demand a left-turn choice while locations in the other half demand a right turn (Figure 4a-b).

Animals were first trained to make left/right turn choices in 20-trial blocks at four different maze locations in the environment (Figure 4a). The maze structure permitted open view to the surrounding large recording room environment which was rich with prominent distal visual cues. After two weeks of such training, individual blocks were shortened to 5 trials and further training ensued to reach criterion performance, at least 9 straight days of above-chance choice-making. Subsequently, animals were exposed to novel environmental locations for the maze to probe learning of the spatial rule (further detail in methods).

To examine behavioral performance, we focused on the 9 days prior to surgery for animals (N=4) undergoing implantation of recording wires and, for those animals not implanted (N=4), a 9-day period subsequent to reaching the criterion described above. Each day, each animal worked through a total of 140 trials arranged in blocks of five

trials with the maze location moved randomly between the four initial locations. A sign test demonstrated that performance for all animals on the task was well above chance (> 90%) for each track location (locations 1-4 of figure 4c; p-values ranged from p = 4.84e-70 to p = 4.54e-56). Thus, animals had robust knowledge of appropriate turn choice according to environmental location of the maze.

It is possible to solve the task for track locations 1-4 by forming four independent place-choice associations rather than by applying a learned, rule-based fragmentation of the environment into two parts. To shed light on the character of the learned spatial relationships and rule out the possibility that rats have formed 4 independent place-choice associations, we tested for transfer of the left- versus right-turning rule to novel positions (locations 5, 6 of figure 4a) within the two sub-regions of the environment.

Remarkably, all 8 rats made the correct choice on their very first encounter with position 5, and 6/8 rats made the correct initial choice at position 6 (figure 4f). Furthermore, the two animals with incorrect choices at position 6 chose correctly on trial 2 and for all but one of the remaining trials of the behavioral session (yellow and black traces). A sign test on all probe trials revealed that first-trial-ever accuracy was significantly above chance (p = 0.004), demonstrating that the learned rule reflects the fragmentation of the environment into subspaces and can be generalized to new circumstances. The choice behavior was inconsistent with a model in which the animal must learn the correct choice at each location independently.

Further ruling out simple, independent place-choice associations, performance accuracy for all animals was significantly worse for track locations 2 and 3 which are closest to the fragment boundary (figure 4c, chi-square test for independence, p-values

ranged from 8.14e-5 to 7.33e-14). This proximity effect reflects increased difficulty of the task when the track location is proximal to the boundary line (dashed line in Figure 4a-b), indicating a continuum of difficulty spanning the whole environment that peaks at the fragment border. If four truly independent place-choice associations were formed and the animals did not fragment the environment, no such continuum would be expected. Furthermore, the task's block structure consisted of five trials in a row at each track location demanding, at the very least, that the animal assess maze location for each first trial of a block. Accordingly, the proximity effect for all animals was exacerbated if only the first trial of each block was examined (see figure 4d,e), an indication that animals may be using a different strategy during the first trial of a block compared to subsequent trials.

3.3.2 Choice Behavior According to Trial Number Suggests Two Choice Strategies

The task structure was such that the first trial of any five-trial block is distinct from trials 2-5. Since the track had just been moved to a different location during trial 1, animals had to know where they were in the room as well as where the track is located in the room, a "track location-based strategy." For subsequent trials of the same block, an animal simply has to repeat a prior action to solve the task if it was previously rewarded, a "prior action-outcome strategy." Alternatively, if an incorrect choice had been made on trial 1, the animal would simply have to make the opposite choice on trial 2.

The behavioral data are consistent with the rat employing these two different strategies. Although all rats performed significantly above chance at each track location (1-4) and for every trial number (1-5), the data showed an obvious trend toward worse performance on trial 1 of each block of 5 trials with better performance on subsequent

trials (figure 4c-f). In terms of performance accuracy, trial 1 is more challenging overall. To statistically assess observed differences between trial 1 and other trials, a chi-square test of independence comparing trial 1 vs trial 2 accuracy was performed. The trial 1 vs 2 accuracy difference was greater than the differences between subsequent trial comparisons (e.g., 2vs3, 3vs4, etc.). Four of eight rats performed significantly worse on trial 1 (significant p-values ranged from $p = 0.02$ to $p = 0.04$), and when considered all together, rats overall performed significantly worse on trial 1 ($p = 2.56e\text{-}7$). Thus, the animals may use a different strategy on trial 1 compared to trials 2-5.

3.4 Discussion

The left/right choice behavior of rats on a T-maze evidenced robust learning of a rule-based environmental fragmentation. All animals proved capable of very quickly (immediately in most cases) applying the behavioral rule learned at four room locations to two new environmental locations. To our knowledge, this represents the first work using decision-making rules to effect an arbitrary division of an environment.

A study by Grieves and colleagues (2016) used a somewhat similar behavioral setup where rats had to solve an odor location discrimination task in each of four identical compartments. In one condition the compartments were each parallel to one another, and in another condition the compartments were fanned out so that each compartment was 60 degrees from one another. Since the correct choice for the odor location discrimination task was different in each compartment, there is a similarity to the current study where the animal had to determine the location of each compartment relative to the other compartments in order to solve the task correctly. The rats in the parallel condition had significantly greater difficulty on this task compared to the 60-

degree angle condition, and many of the animals didn't even reach criterion. Although there are some similarities, in the present study the animals complete the task on a track in an open environment, so that on each trial all of the same distal cues are visible to the rat and clue the animal into the track's location. This may explain the discrepancies between our results and those of the multi-compartment task.

In the present task, animals showed significantly lower accuracy on trial 1 compared to subsequent trials in a block. This difference in performance on trial 1 vs subsequent trials, and the five trials per block structure of the task raises the possibility of alterations in the strategy used to determine choice on trial 1 compared to subsequent trials. Such a robust behavioral distinction between trial 1 and trials 2-5 implies two strategies are used by the rat depending on recent experience at a track location: 1) a trial 1 'track location based strategy' in which the rat needs to know its allocentric room location; and 2) a trial 2-5 'prior response strategy' in which the rat simply needs to execute the same procedure as in the prior trial, if rewarded, or the opposite procedure if not rewarded. The prior response strategy could seemingly take advantage of such encoding of recent history, but would not require any knowledge of room location for decision-making.

There is precedent for different strategies used by a rat in a different cross maze paradigms depending on how long they've been performing the task (Chang & Gold, 2003; Tolman, Ritchie, & Kalish, 1946; 1947; Packard & McGaugh, 1996; Packard, 1999). These tasks usually involve a cross maze placed in the same location over multiple trials, where rats start from the same arm (e.g. south arm) and turn toward a baited arm. During a probe trail, to determine strategy, the animal starts from the opposite arm (e.g.

north arm). Generally, the animals will initially use a place strategy (turning toward the correct location in the room), but eventually over time will switch to a response strategy (turning in the egocentric direction that they usually turn, left or right). In our task, the track switches locations altogether at the start of every block, and so a track location based strategy established by the entire track's placement in the room would need to be used at the start of each new block.

With the difference in performance on trial 1 vs subsequent trials, paired with distinct possible strategies across the different trial types, it follows that there may be some extra difficulty in the first trial decision-making inherent in the structure of the task, perhaps due to greater demand on retrieval mechanisms or heightened task engagement on the first trial of a block when the track location has just been shifted. For any first trial, the rat must pay greater attention to its location in the room in order to determine a correct turn decision since repeating the decision from a prior trial at another room location would yield only chance-level performance (50% correct), as the animal is equally likely to be placed in a left-turning vs. a right-turning case. In the present study, the accuracy was above chance for all trials and track locations.

The difference in behavioral accuracy between trial 1 and subsequent trials raises the possibility that neural activity might distinctly reflect the two strategies in some way. The use of different strategies over time (place and response) is associated with different neural systems (Chang & Gold, 2003; Packard & McGaugh, 1996; Packard, 1999). Several findings in the literature suggest that HPC activity can track the recent history of exposure to a given environment and decision-making context (Colombo, Brightwell, & Countryman, 2003; Wimmer & Büchel, 2019). Additionally, changes in HPC theta

rhythm have been reported for animals exploring novel environments (Feng, Silva, Foster, 2015; Penley et al., 2013; Jeewajee, Lever, Burton, O'Keefe, & Burgess, 2008). The neural activity patterns of HPC and PPC as a function of trial number for the present task is measured and discussed in the next chapter.

Chapters 3 and 4, in part, have been published in *Neurobiology of Learning and Memory,* Shelley, L.E., Barr, C. I., & Nitz, D.A. (2022). The author of the dissertation is the primary author of this publication.

Chapter 4: Experiment 3 – Cortical and Hippocampal Dynamics Under Logical Fragmentation of Environmental Space

4.1 The Present Study

Navigation in humans and animals is often constrained to movement along pathways that are interconnected and oriented in either a simple or complex fashion. The layout of paths, their interconnections and affordances impact human perception and navigational problem solving (Warren, Rothman, Schnapp, & Ericson, 2017), as well as neural activity in hippocampus and cortex in humans moving through virtual environments (Bonner & Epstein, 2017; Javadi et al., 2017) and in animals moving through physical environments (Nitz, 2006; Ainge et al., 2007; Grieves et al., 2016; Gupta et al., 2012; Dabaghian, Brandt, & Frank, 2014). A frequently-recurring, fundamental navigational problem in such environments, whether regular (e.g., Manhattan or Fresno, CA) or irregular (e.g. Boston or Arlington, VA) in their arrangements, is the decision whether to turn left or right as one approaches an intersection. Like humans, animals routinely encounter this same problem multiple times within a single environmental setting, as their movement is often constrained to naturally occurring pathways, pathways within urban environments, or tunnel systems below the surface. In all cases, the choice at each intersection must take into account the unique context associated with it.

Choice behavior and neural activity leading up to choices at isolated "T" junctions has been studied extensively using the T-maze, Y-maze, or a squared figure-8 maze. Multiple studies suggest that part of the solution to a turn-choice navigational problem is achieved through hippocampal (HPC) trajectory-specific encoding of absolute location in

an environment (Pastalkova, Itskov, Amarasingham, & Buzsáki, 2008; Wood et al., 2000; Grieves et al., 2016; Ferbinteanu & Shapiro, 2003; Ainge et al., 2007; Frank et al., 2000). Here, in addition to the well-known mapping of absolute location (or "place") in an environment, HPC patterns discriminate different trajectories taken through the same places on 'Y' and 'T' shaped mazes.

In complement to trajectory-dependent encoding of environmental location in HPC, posterior parietal cortex (PPC) neurons also map position in a trajectory, but this mapping is independent of environmental location (Nitz, 2006; Nitz, 2009; Nitz, 2012). That is, specific, spatially-tuned firing patterns for PPC neurons recur when the same trajectory is traversed between different start and end points in the environment and is associated with different, even opposite, directions of travel. In the same PPC neuron populations, a large minority (~30%) of PPC neurons exhibit differential firing during left versus right turning behavior (Whitlock et al., 2012; Nitz, 2006; McNaughton et al., 1994; Wilber et al., 2014). However, route-position mapping of individual neurons and PPC populations is not epiphenomenal to these action correlates (Nitz, 2006; Nitz, 2009; Nitz, 2012; Whitlock et al., 2012; Wilber et al., 2014). This indicates that PPC produces a combined action and route-position encoding that could be used to guide action selection (left versus right turning) according to perceived location along a complex route that passes through multiple intersections.

Both lesion and recording studies have suggested that HPC and PPC interaction is critical for navigation (Rogers & Kesner, 2007; Save, Paz-Villagran, Alexinsky, & Poucet, 2005; Qin et al., 1997). But, exactly how these regions interact to guide navigational decision-making remains to be determined. In fact, outside of recording

experiments performed under head restraint and virtual reality (Harvey, Coen, & Tank, 2012; Krumin, Lee, Harris, & Carandini, 2018), the spatial tuning and trajectory-dependence of PPC neurons during T-maze performance is unknown. What is clear is that the PPC encoding of route position also reliably encodes proximity to an upcoming intersection (Nitz, 2006). In principle, then, PPC ensembles can set a framework for left/right-turn decision-making that generalizes to all physical instances of T junctures within an environment. Structures such as hippocampus, subiculum, and retrosplenial cortex could provide information on environmental position and orientation that, as direct or indirect inputs to PPC, could guide choice-making at individual locations. Finally, PPC projections to secondary motor cortex could provide a final pathway to implement actual navigational actions (Yamawaki, Radulovic, & Shepherd, 2016; Nitz, 2009; Olson, Li, Montgomery, & Nitz, 2020).

For environments containing multiple, spatially distributed choice-points, a further consideration concerns fragmentation of the environment into neighborhoods. Turn choices that get one to a goal will often cluster in different fragments of an environment. For instance, if walking north in one neighborhood, the good restaurants might be to the west and so a left turn will suffice at any of multiple intersections, but if one walks a bit farther north into another neighborhood, the good restaurants might be to the east and require a right turn at any of the intersections. Finally, in addition to a spatial context, each individual T-intersection has an experiential context where, upon first approach, the person or animal must define where he is and make the appropriate left or right turn, but with repeated experience turn choice may be a more automatic procedure not requiring knowledge of spatial location.

To begin to address such forms and contexts for navigation, we developed a T-maze spatial decision-making task that required animals to know in which half of a room they were located. Under these conditions, we find that HPC and PPC spatial firing patterns are aligned to the same track-based frame of reference, as opposed to a room-based frame, and that recent experience significantly impacts the magnitude of spatially tuned firing rates. The findings call attention to the impact of experience in decision-making and call for revision of current models for T-maze choice behavior in complex environments.

4.2 Methods

4.2.1 Subjects

Adult male Sprague Dawley rats (Harlan Laboratories) approximately 6 to 12 months of age were used as subjects (n = 8). The rats were housed individually in standard plastic cages and kept on a 12-hour light-dark cycle. Animals were maintained on a food-restricted diet (85-95% of free-feed weight) to motivate them to perform the task. All animals were habituated to the colony room and handled for 30 minutes to 1 hour each day for 1-2 weeks prior to task training. All experimental protocols adhered to AALAC guidelines and were approved by IACUC and the UCSD Animal Care Program.

4.2.2 Apparatus

The behavioral task was conducted using a T-shaped track with a round start-plate (18.5cm diameter) at the base. The track was 122 cm long x 10 cm wide on the stem and 67.5 cm long x 10 cm wide on the top. A 0.5 cm tall railing enclosed all sides, allowing the animal to see the larger room and distal cues on the walls.

4.2.3 Behavioral Training

Animals were trained to traverse the stem of the T-shaped track and make either a left or a right turn at the choice point for a food reward. Correct left or right choices depended on the track's position in the room in relation to an implied, rule-defined boundary (figure 4b). The animals then made a return run, retracing their outbound trajectory directly back to the start plate. Only correct turns on outbound runs were rewarded, and rats received a smaller reward for inbound runs to motivate prompt returns to the start plate. Animals were trained to run in a ballistic fashion to eliminate pauses that would influence analysis of spiking data. There was no visible, physical line drawn dividing the room. Animals were able to localize themselves by reference to prominent, fixed distal cues in the 304 cm x 457 cm recording room. Track locations were placed 20 cm apart for locations 1-5 and position 6 was located 10 cm adjacent to position 1 (figure 4a). Track location distribution spanned most of the length of the room. Fixed distal cues included large wall murals, a desk, a table, and the recording rig, all distributed around the perimeter of the room.

Initial training involved only track sites 1-4 in larger blocks of 20 trials in each location in randomized order. During a block, the track was placed in one of the 4 locations, and then moved to another location at the start of the next block. Track locations were in randomized order. Rats learned through trial and error that track locations 1 and 2 required left turns and locations 3 and 4 required right turns. After 2 weeks of 20-trial blocks, the task structure was broken up into 28 blocks of 5 trials each and performance accuracy was recorded (figure 4a).

Once rats met criteria on track sites 1-4 (significantly above chance and at least 9 days of behavioral results), track location 5 was introduced as a probe trial, with the

exception of one rat that was tested on track location 5 before meeting criteria (figure 4a). This served to rule out simple individual associations between place and a correct action and assess for transfer of the whole-room fragmentation to novel positions. Once animals performed significantly above chance on positions 1-5, track location 6 was introduced as a second probe trial (figure 4a). Novel track locations were immediately incorporated into the 28-block structure.

4.2.4 Surgery

Once trained, 4 of the 8 rats were surgically implanted with tetrode arrays (bundles of four 12 μm tungsten wire, gold-plated to impedances of 0.1 mOhms) mounted to custom-built microdrives that allowed for ventral movement in 40 μm increments across days. Isoflurane (4-5% induction, 1-2% maintenance) was used to anesthetize animals for surgery and they were placed in a stereotaxic apparatus (Kopf Instruments). Craniotomy and resection of dura mater over the PPC was performed to allow bilateral implantation of microdrives over the right and left posterior parietal cortex (anterior-posterior: 4mm posterior to bregma, 2.3mm lateral to the midline suture, .5mm depth from brain surface; Paxinos & Watson, 2007).

4.2.5 Recordings

The recording techniques necessary for the current project have been used and described in detail in published work from the Nitz laboratory (Alexander & Nitz, 2015; Nitz, 2012). Recordings of multiple single neuron ensembles and local field potentials were obtained from both PPC and the CA1 area of the HPC during track traversal. Data was collected on a 48-channel Plexon system that coordinates signal amplification, filtering, and sampling of action potential waveforms. In each recording, action potentials

were amplified at the headstage connection (20X, Triangle Biosystems), the pre-amp stage (50X), and at the amplifier stage (1-15X). Signals were bandpass filtered (450 Hz – 8.8 kHz). Spike waveforms were digitized using SortClient (Plexon, 40 kHz sampling).

The microdrives were built to allow dorsal to ventral (PPC to HPC) movement of tetrode bundles at 40-micrometer intervals, affording recordings of many neurons in one animal across days in both PPC and HPC. The transition from PPC into HPC is routinely recognized at first by relative silence across electrodes (when wires are within the corpus callosum) and subsequently by the emergence of sharp wave ripple events in the local field potential that occur when the animal is immobile. Recognition of such events is critical to fine tuning the timing of wire movement into the relatively thin CA1 layer. Each rat had 3 microdrives with 4 tetrodes per microdrive allowing recording from all 48 channels.

Recording sessions had the same 28-block structure as training sessions. Overhead cameras 2.6 m above the floor recorded the animal's position on the track using Cineplex software (Plexon Inc., Denison, Tx) while rats performed the task. Cineplex detects differently-colored LED lights attached to the rat's implant and encodes position in the room. Aside from spatial positions, variables that can be extracted from this data include direction of movement, head orientation, velocity, and left and right turning action. Tracking data was filtered for ballistic runs such that pauses would not influence analysis of spiking data.

4.2.6 Histology

Animals were perfused with 4% paraformaldehyde under deep anesthesia after all recordings were completed. Brains were extracted, sliced into 50 μm sections, and Nissl

stained to reveal wire locations and final depth in PPC and HPC. Nissl stains confirmed wire locations and final wire depth in PPC and CA1 (figure 5; tracks drawn represent beginning and ending of recording locations). Final depths were cross-referenced to logs of turning depth for each bundle, to records noting the first day in which theta-frequency (8Hz) activity was found (a feature of most hippocampal neurons), and to records noting the first day that sharp-wave ripple events were observed (an indicator of close proximity to the CA1 pyramidal layer).

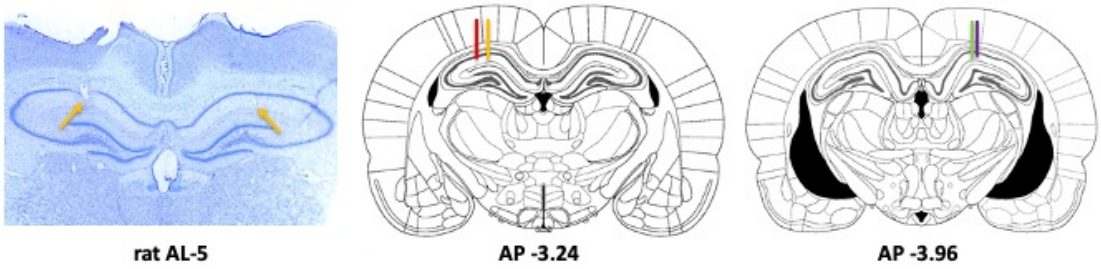

Figure 5. Recording wire tracks through posterior parietal cortex and hippocampal sub-region CA1. Left panel depicts typical Nissl stained coronal slice used to define the deepest level of penetration of tetrode wire bundles. Orange arrows mark the location of recording wire tracks. The recording track on the right side is more apparent in adjacent slices. Middle and right panels depict the space over which tetrode wire bundles progressed across recordings from beginning to end. Each color corresponds to one of the recording animals. Note that tetrode bundles are taken to a depth of 0.5 – 0.7 mm from the surface of the brain during surgery.

4.2.7 Identification of Clean, Ballistic Track Traversals

Tracking data was loaded into a custom-made MATLAB user interface to mark individual trial starts and ends and to evaluate whether each run was clean and ballistic (i.e. having uninterrupted locomotion). Trials were automatically categorized into track locations (1-4) as well as correct vs incorrect using a custom-made MATLAB script. Only clean and accurate runs were included in neural recording analyses to prevent confounding reward time periods, stalled runs, incorrect turn choices, and between-run

time periods with neural activity. PPC is sometimes sensitive to action, and HPC patterns can change as rats exhibit exploratory, head-scanning behaviors (Monaco et al., 2014). Therefore trials where the rat paused its run for any reason were not included in analyses. Clean traversals were each approximately 2-3 seconds long on average.

4.2.8 Linearized Firing Rate Calculation

To characterize firing activity during track traversals, individual action potentials were mapped to specific positions on a template generated from the animal tracking data. A spatial template match for the average movement of the animal in pixel space was generated using custom MATLAB software. Trials were individually plotted and starts, ends, and turn apices were marked, and a series of 1.49cm template bins were generated across the animal's trajectory. Positional firing rate vectors for inbound and outbound runs were then constructed by dividing the total number of spikes in each template bin by the total occupancy time in each bin on each path traversal. Individual firing rate vectors varied in length across recordings due to differences in the precise trajectories taken by animals. Therefore firing rate vectors were interpolated (MATLAB 'interp1' function) to the average template length in bins across recordings (98 bins). Mean cross-trial positional firing rate vectors were calculated from these vectors for individual trials (see fig 6a-b). These positional firing rate vectors allow identification spatial firing fields or action correlates, where neuronal activity reliably and robustly increases. Such positional firing rate vectors can be combined to assess firing patterns for the whole population of neurons in a given area across positions.

4.2.9 Unit Isolation

Plexon's Offline Sorter software was used to isolate units. Peak minus valley values of the waveform for each spike were plotted from different tetrode wires on the X and Y axes, then spikes that formed clusters were selected as main units. Noise was then reduced by plotting various waveform features for each spike including energy, nonlinear energy, and principal component projections. Spikes that separated from the main cluster were trimmed away.

4.2.10 Filtering Out Interneurons

HPC interneurons were not included in analyses. For each HPC neuron, all bins where the firing rate was below 0.3Hz were located. If a neuron had fewer than ten bins (out of 98) with firing rates below 0.3Hz, it was considered an interneuron and filtered from the dataset.

4.2.11 Correlation Matrix Construction

Correlation matrices were created for the firing rate vectors of the population of PPC and HPC neurons to compare track locations (1-4; figure 10a-b). As done in other works (Alexander & Nitz, 2015; Cowen & Nitz, 2014), these correlations were used as a metric for similarity in spatial mapping rather than for statistical testing. To construct these, the firing rates of all neurons at a particular position bin for a particular track location was correlated with the firing rates of all neurons at a particular position bin for a different track location. All pairwise combinations of bins were correlated for two different track locations and put into a correlation coefficient matrix where they can be easily visualized. Matrices were created for all pairwise track location comparisons (1-4). From such matrices the extent to which HPC or PPC ensembles exhibit similar firing

patterns across track locations can be determined, where higher correlation values represent position bins that were mapped more similarly at the two track locations.

4.2.12 Choice Probability Analysis

To compare firing rates between trials (1-5) and firing rates between track locations (1-4) on a per-run, per position bin basis, choice probability analyses were conducted for pairwise trial and track location comparisons (figure 6d & 9c). This analysis was adapted from Britten et al. (1996) and the calculations involved are equivalent to the area under the curve of the receiver operating characteristic (figure 6c). Choice probability values are an indicator of how strongly each neuron's firing rate predicts trial number or track location (and therefore a rat's eventual choice of a left- vs right-turn).

Firing rate vectors for each run were first smoothed by calculating a moving average of each vector with a rolling subset of 5 position bins. Then for each pairwise comparison (trials 1-5 or track locations 1-4), a Mann-Whitney U statistic was calculated for each neuron at each position bin average. An area-under-curve (AUC) statistic was calculated from this for each of the distributions of firing rate values at each position bin average. The resulting two AUC values for each pairwise comparison are inverses of each other across chance (50%; if one is 40% the other is 60%), but we were only interested in the magnitude of the prediction, not the direction. Therefore, the maximum AUC was taken at each position bin average and put into a vector of that neuron's choice probability at each position bin average, allowing easy visualization of the time course of how strongly the neuron predicts either trial (figure 6d) or track location (figure 9c) at each bin. These values were then compared to shuffled data from a bootstrapping

procedure where run labels for each comparison type (trials 1-5 or track locations 1-4) were shuffled.

As a behavioral control for these values, choice probabilities for each bin were calculated in the manner described above for head direction as well as velocity to assess whether behavioral changes at each bin predict either trial or track location (and therefore the rat's eventual turn choice).

4.2.13 Analysis of Local Field Potentials

Eight HPC recordings were selected for analysis, two random HPC recordings from each of the four recording animals. One LFP channel was selected per recording. In each case, the channel selected was from the nearest available wire to recorded HPC neurons, provided the signal subjectively appeared noise-free. Raw LFPs were band-pass filtered in MATLAB for theta rhythm (6-10hz). Theta filtered LFPs were then rectified and an amplitude envelope trace connecting the peaks of the rectified trace was calculated. Only portions of signal whose time stamps corresponded with animals running trials on the task were used for analysis. T-tests comparing trial types were conducted using mean envelope values for each run.

4.3 Results

4.3.1 Hippocampal and Parietal Firing Patterns Differentiate First Trial of a Block

As stated, choice accuracy was significantly above chance levels for all conditions, but overall accuracy was significantly worse on trial 1 of each block, indicating rats may be using a different strategy on the first trial compared to subsequent trials. We therefore conducted separate analyses of spatial tuning in HPC and PPC

populations according to trial number to see if HPC or PPC patterns are sensitive to the more challenging decision-making on trial 1.

The behavioral indication of different strategy use on trial 1 vs trials 2-5 was paralleled by differences in both HPC and PPC spatial firing patterns. Figure 6 (a-b) depicts positional rate vectors for example HPC and PPC neurons. Rate vectors for some HPC neurons evidenced higher firing and earlier onset of firing on trial 1 (red traces) relative to trials 2-5 (black traces). The HPC cell of figure 6a has a place field over a portion of the stem, and trial 1 firing (red traces) occurred earlier and at higher rates than subsequent trials (black traces). The PPC cell (figure 6b), consistent with prior literature, is less sparse in its firing but generates a reliable, if irregular, pattern across trials (1-5; red vs black traces). Remarkably, both PPC and HPC neurons exhibit repeated firing patterns despite the different track locations (1-4; each firing rate vector depicted in figure 6a-b), a finding we explore in the next section.

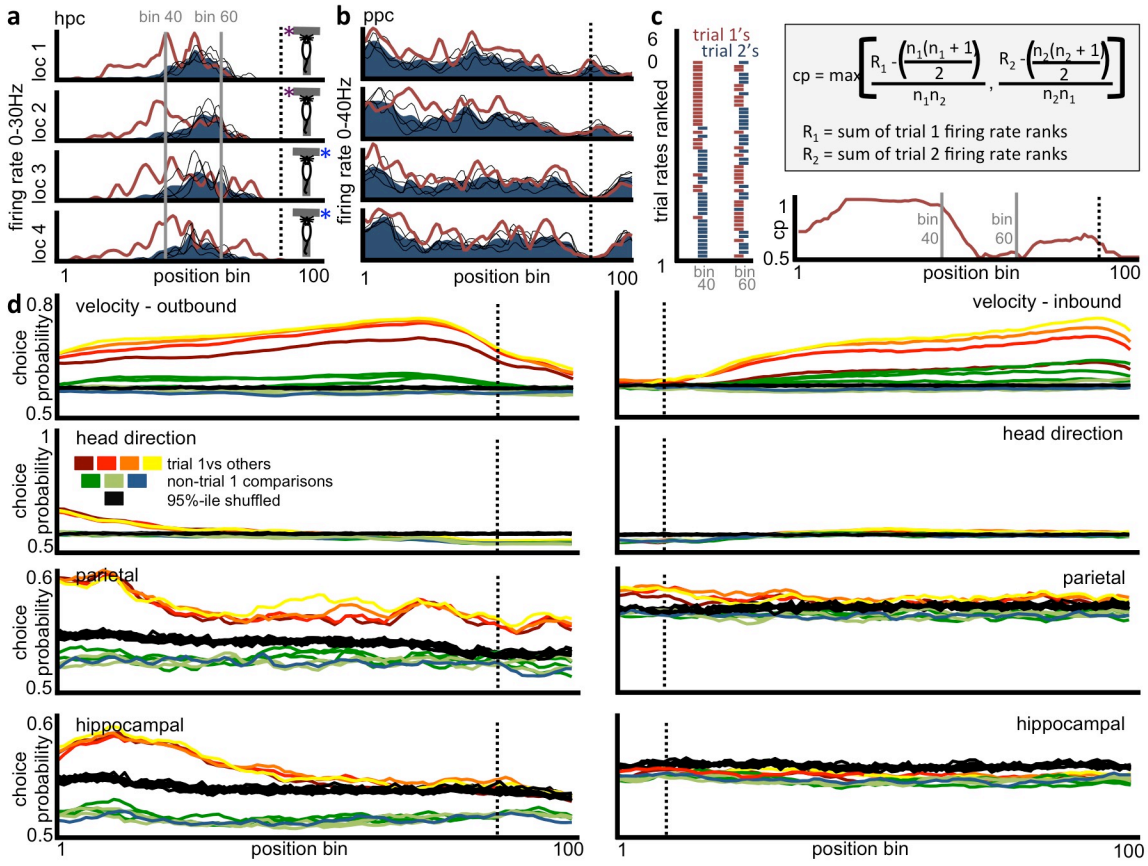

Figure 6. Firing patterns differentiate trial 1 of a block. (a-b) Outbound firing rates of an example hippocampal (a) and parietal (b) neuron. Each of the four plots shows firing rate vectors for one location (1-4). Red trace shows mean firing rates for trial 1 only. Black lines indicate mean firing rates for trials 2-5. Mean firing rates for all trials combined shown in blue shaded area. Black dashed line indicates turn location. T-shaped track, rat and turn direction for each location depicted to right of HPC rates. Gray lines demarcate position bins 40 and 60 which each show a large (bin 40) and small (bin 60) difference between trial 1 and subsequent trial firing. **(c)** Choice probability analysis example. Left: Per-run ranks of firing rates at bin 40 and bin 60 from HPC example neuron in (a). Trial 1 shown in red, trial 2 shown in blue. Upper right: Choice probability equation. Lower right: Trial 1 vs 2 choice probability trace for HPC example neuron in (a). Gray lines demarcate bin 40 and bin 60. Dashed line demarcates turn location. **(d)** Trial choice probability plots. Outbound and inbound mean choice probability plots for velocity, head direction, PPC firing rates, and HPC firing rates. Warm colors represent pairwise trial 1 vs other trial (2-5) comparisons (1v2, 1v3, etc). Cool colors represent pairwise non-trial 1 comparisons (2v3, 2v4, etc). Black lines indicate 95th percentile of choice probabilities from shuffled data. Dashed black line indicates turn location.

To analyze this first trial effect across all HPC and PPC neurons, a choice probability (CP) analysis was conducted (figure 6c). This analysis was adapted from

Britten and colleagues (1996) and the calculations involved are equivalent to the area under the curve of the receiver operating characteristic. Essentially, we used it as a measure of the degree to which a neuron differentiates two conditions (e.g. trial number) at each position bin along the track on a per-run basis. Based on the observed rate differences for two conditions, the CP measure reflects the probability of correct assignment to a condition for any new value. A schematic describing the CP analysis using firing rates from the example neuron depicted in figure 6a is shown in figure 6c. For any given track bin position, the firing rates of a single neuron at that bin for every run in the two conditions (e.g. trial 1 and trial 2) are ranked (Figure 6c: red/trial 1 vs blue/trial 2 tick marks in left panel show ranks for every run for neuron depicted in figure 6a, at position bins 40 and 60 demarcated by gray line in Figure 6a). The rankings are summed for each group and are then compared using the equation given in figure 6c. CP comparing two trials is calculated for every track bin (e.g. the resulting example CP trace for this neuron at these two position bins is shown in figure 6c: bottom). Mean CP values across neurons were then calculated (figure 6d, parietal and hippocampal colored traces) and compared to the 95th percentile of mean CP values for 1000 different randomizations of trial identity for the same data (figure 6d, parietal and hippocampal black traces). These same calculations were also performed for velocity, and head direction (figure 6d).

Across neurons, CP values for outbound runs for both HPC and PPC populations differentiate the first trial of a block from other trials (figure 6d). All trial 1 versus trial 2-5 mean CP values (yellow-red traces, N=339) for PPC outbound runs lie above the 95th percentile (black traces) for mean CP values when trial identity (trial 1 data included) was randomized. This was also true for nearly all mean CP values for HPC prior to the T-

maze intersection (yellow-red traces, N=260). No trial differentiation beyond chance was found for comparisons using trial 2-5 pairings (green-blue traces). If neurons did not differentiate two conditions, we would expect CP values to exceed the 95 percentile of shuffled data for only 5 percent of all track positions. In contrast, inbound runs do not show differentiation amongst trials (figure 6d, right), a result we expected since all inbound runs involve running back to the start plate with no allocentric spatial task to solve, no matter which trial.

To examine behavioral differences during trial 1 as a possible explanation for the firing rate differences, trial CP was also calculated for head direction and velocity (figure 6d). Here, CPs beyond the 95^{th} percentile of CPs from shuffled data would indicate that the animal's head direction or speed might explain firing differences in HPC or PPC firing rates between trials. Although there is trial 1 differentiation in the velocity (outbound and inbound runs) and head direction (outbound runs only) of the animal, the envelope of the effect does not fall in step with the firing rate CP traces of HPC and PPC. Velocity differences are apparent throughout the track space. For outbound runs, head direction differences between trials are observed very early in the run but return to meet the CPs from shuffled data over later sections. HPC and PPC trial 1 differentiation in firing rates is not maintained on return runs while velocity differentiation is, ruling out an explanation based on speed. Head direction CP also differentiates the first trial on outbound runs. However, this differentiation disappears early in the run and does not exist on inbound/return runs. Overall, the pattern of head direction CPs does not follow the envelope of firing rate CP traces, precluding a complete explanation based on the animal's head direction.

There are several factors that could differentiate trial 1 firing in HPC and PPC on outbound runs including: 1) Reliable increases and decreases in rate that vary by neuron (consistent with an overall rate remapping); 2) Overall bias to increased or decreased rates across the population of neurons; 3) Changes in peak firing rate; or 4) A shift or lag of the positional firing rate envelope. Other possibilities include more systematic changes (e.g., only positive or negative changes) in mean rate, peak rate, or forward (or backward) shifting. We note here that CP values do not imply higher or lower firing, only a differentiation; CP reflects the degree to which a neuron's firing rates differentiate two factors (i.e trials), without heed to which factor is associated with higher vs lower rates. An overall rate increase, a bi-directional rate remapping, or a change in lag of a place field (either bi-directionally or in one direction systematically) all could differentiate trial 1 from another trial on CP.

Therefore, to further analyze the nature of the firing rate differentiation between trials for outbound runs, we examined the outbound rates themselves to find any bias in the direction of change from one trial to another. Figure 7a shows overall mean firing rate across all neurons for trial 1 (red) compared to trials 2-5 (blue) for HPC and PPC neurons, inbound and outbound runs. From figure 7a, it appears that outbound HPC rates are higher overall across neurons for trial 1 compared to other trials. PPC outbound rate differences that were observed in figure 6d appear less consistent in direction when examining across neurons in figure 7a. Inbound rates for both HPC and PPC do not look different across trials, consistent with the CP result in figure 6d. A Wilcoxon rank-sum test was conducted to examine mean rate differences across all neurons and positions for each pairwise trial comparison for outbound runs. Overall mean rates were significantly

higher for trial 1 compared to means for all other trials (2-5) for HPC neurons during outbound runs, with trial 1 firing 12% higher than trial 2 (figure 7b upper bar plots; p-values for comparisons involving trial 1 outbound ranged from p = 4.47e-10 to p = 1.03e-10; p-values for non-trial 1 comparisons were statistically non-significant and ranged from 0.08 to 0.85). Far less evidence for change in overall rates across trials in a block was observed for PPC (figure 7b, lower bar plots), with the largest significant difference in firing rate (trial 1 vs 3) at 1.7% (p-values ranged from p = .007 to p = .820, with only 3 comparisons yielding significant differences: trial 1vs2, 1vs3 and 3vs4).

Figure 7b shows a cumulative distribution of mean HPC firing rates for all positions and neurons on trial 1 (red trace) compared to trials 2-5 (blue traces). The axes of this plot were adjusted to emphasize the difference between the distributions; not shown are the forty-five percent of all HPC positional firing rates at zero. We note that the number of zero rates was evenly distributed across different trials ranging only from 44-45%. As depicted, the axes cut off 35% of the lower end of the distribution (all zero rates) and 0.2% of the higher end of the distribution (rates above 35hz). Between these extremes, first trial rates are shifted toward higher values relative to trials 2-5.

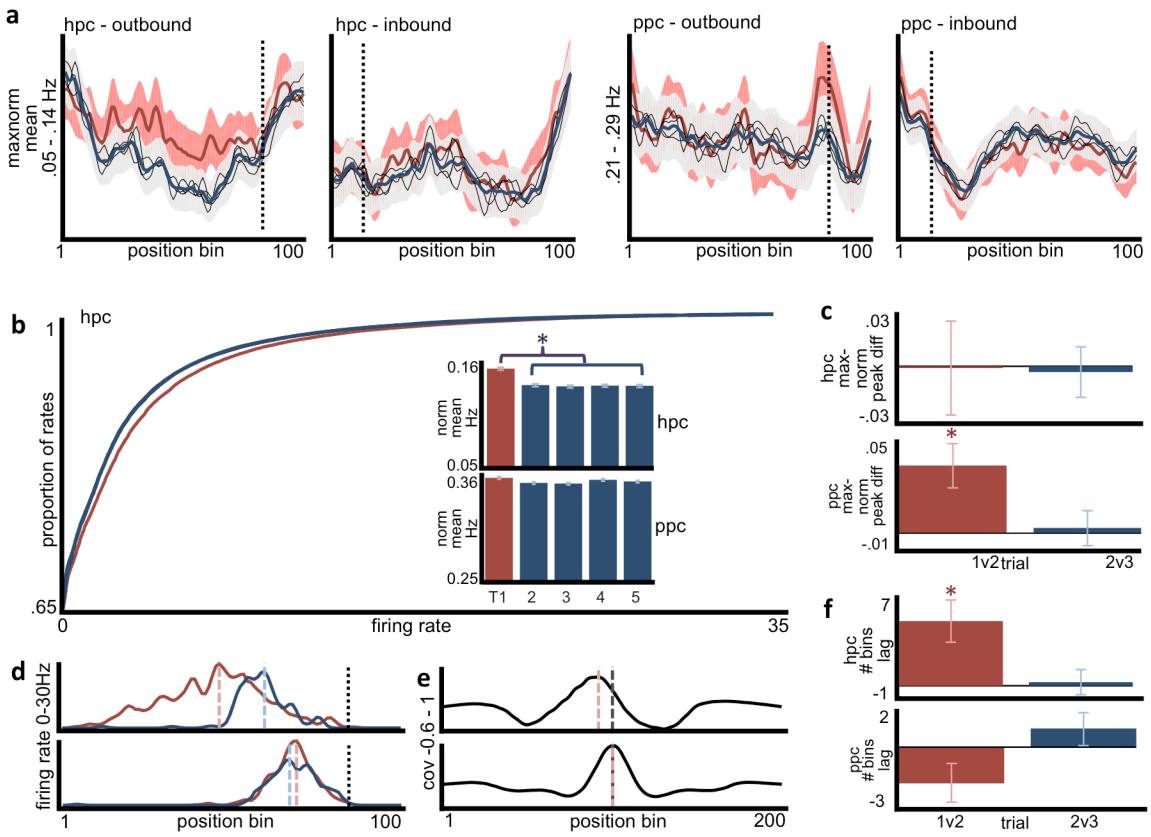

Figure 7. HPC firing patterns exhibit higher rates and earlier firing during trial 1 of a block while PPC patterns exhibit rate remapping. (a) All neuron max-normalized mean firing rates for trial 1 vs other trials. All neuron mean trial 1 firing rates shown with dark red trace with +/- standard error shown in light red shading. All neuron mean trials 2-5 firing rates shown in blue with +/- standard error shown in gray shading. Each individual trial 2-5 trace shown in black. Black dashed lines represent turn location. **(b)** Overall mean comparison. Cumulative distribution of all trial 1 rates (red trace) and all trial 2-5 rates (blue trace). Bar graphs depict overall mean firing rate for each trial 1-5 for HPC (upper) and PPC (lower) with standard error bars. **(c)** Bar graphs showing trial 1vs2 (red) and 2vs3 (blue) peak firing rate differences (max-normalized) with standard error bars. **(d)** Mean firing rate traces for example HPC neurons. Trial 1 mean firing rates indicated by red trace, trial 2 by blue trace. Light red and blue dashed lines show field peak locations. Black dashed line indicates turn location. Upper: HPC example with lag between trial 1 and trial 2 peaks. Lower: HPC example with little to no lag between trial 1 and trial 2 peaks. **(e)** Spatial cross-correlation comparing trial 1 and trial 2 of example neurons. Black trace shows spatial cross-correlation between trial 1 and trial 2 of example neurons in (d). Black dashed line shows center point of cross correlation. Light red dashed line shows peak of cross correlation. Upper: offset of peak from center shows offset between trial 1 and trial 2 fields with trial 1 firing earlier on the track. Lower: overlap of peak from center shows no offset between trial 1 and trial 2 fields. **(f)** Bar graphs showing trial 1vs2 (red) and 2vs3 (blue) mean lag between peak and center of cross correlation with standard error bars.

Consistent with the lack of overall change in mean rates for PPC neurons, the cumulative distribution plots for PPC showed no clear difference between any trial number. Trial 1 differentiation by PPC demonstrated in the CP analysis, therefore, was due to a rate remapping of individual neurons rather than an overall rate increase across the population of neurons as in HPC.

The cumulative distribution plots of all positional firing rates indicates that the HPC neuron rate changes detected by CP analysis occur across a wide range of rates. Nevertheless, to examine if trial differences were due mainly to peak firing rate differences rather than overall differences in non-maximal parts of a firing field, a Wilcoxon signed-rank test was conducted on peak rate differences for each pairwise trial comparison. None of the ten HPC trial-versus-trial comparisons were significantly different with a less than 1% change from trial 1 to trial 2 (figure 7c, upper, shows trial 1vs2 and 2vs3 peak differences; P-values for all comparisons ranged from $p = 0.32$ to $p = 0.97$), indicating that trial 1 differentiation was due to non-maximal parts of HPC positional rate vectors. However, peak firing rate comparisons between trial 1 and trials 2-5 were all significantly different for PPC (p-values ranged from 0.0008 - 0.002; figure 7c, lower, shows trial 1vs2 and 2vs3 peak differences). Conversely, no comparison among trials 2-5 reached statistical significance for PPC (p-values ranged from 0.555 - 0.927). Thus, trial 1 differentiation in PPC seems largely due to changes in maximal parts of the firing patterns, rather than systematic overall mean increases or decreases.

Lastly, a possible shift or lag in place fields was examined by calculating a spatial cross correlation of rate vectors for different trials. The offset, or lag, of the peak from the center point in these cross correlations was taken as a measure of the extent to which the

field has shifted or extended forward or backward on the track between trials (figure 7d-e). Figure 7d shows firing rate vectors for two example neurons with trial 1 trace depicted in red and trial 2 trace depicted in blue. The top neuron shows a lag between the peaks of trial 1 and trial 2, while the bottom neuron shows a much smaller difference between the peaks. Figure 7e shows the corresponding cross correlations between trial 1 and trial 2 traces for these neurons. The lag between the peak position bin and center of the cross correlation was calculated and averaged across neurons (figure 7f). A Wilcoxon signed-rank test conducted on the lags revealed that HPC fired significantly earlier for trial 1 vs trial 2, 3, and 4 outbound runs (figure 7f, upper shows trial 1vs2 and 2vs3 lags). The trial 1 vs 5 comparison was not significantly different despite similar direction and degree of change. P-values for trial 1 comparisons ranged from $p = 0.0006$ to $p = 0.1$. Of the non-trial 1 outbound comparisons, only trial 2 vs 4 was significantly different ($p = 0.002$), but with a smaller lag change than for all trial 1 comparisons. A Wilcoxon signed-rank test for PPC revealed no significant differences in peak lag between trials (figure 7f, lower shows trial 1vs2 and 2vs3 lags; p-values ranged from 0.181 to 0.950).

As already considered theoretically and determined behaviorally, trial 1 outbound runs are a better test of the rat's ability to use a track location-based strategy to solve the task. HPC and PPC neuron dynamics differ on the first trial in a systematic fashion, and may reflect increased task engagement on trial 1 compared to subsequent trials. Inbound runs do not involve solving an allocentric task, as the animal runs back to the start plate every time no matter the track location in the room, so we would not expect the neural representation of inbound runs to differentiate trial number. Despite differences in the form of positional firing rate changes for outbound HPC and PPC (mean rates vs peak

rates vs field shifts), dynamics in both regions support the idea that the animal has incorporated a schema of the full spatiotemporal structure of the task into its behavior and its neurophysiological mapping. Neurophysiologically, this takes the form of overall increased rates and a spatial shift of firing for HPC. Neither was seen in PPC indicating that trial differentiation in parietal CPs reflects balanced increases and decreases of rate over a stable positional firing pattern (i.e. rate remapping).

4.3.2 Hippocampal Theta Rhythm Differentiates First Trial of a Block

To further examine the trial effect described in the previous section, we also analyzed the population activity given by the HPC theta rhythm in local field potentials (LFP). HPC spiking activity is temporally organized by the theta rhythm (O'Keefe & Recce, 1993; Dragoi & Buzsáki, 2006), which raises the possibility that the theta rhythm, as a measure of population level dynamics, could differentiate trials along with the units.

Eight hippocampal recordings were selected for analysis (2 randomly chosen from each animal). Raw LFPs were filtered for theta (6-10hz) and theta amplitude envelopes were calculated as described in methods. Figure 8 shows envelope means (colored dots) for each trial for all 8 recordings, all normalized to trial 1 to emphasize the change in amplitude on average from trial 1 to subsequent trials. Each animal is depicted by a color; the darker shade depicts one recording from that animal, while the lighter shade represents another recording from that animal. The black trace represents averages across all four animals based on one of the two recordings from each animal. The gray trace depicts averages across each animal for each of the other recordings analyzed (essentially two "samples" across all animals).

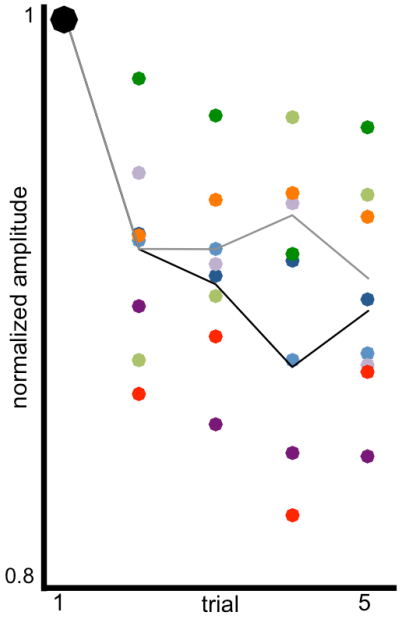

Figure 8. Mean normalized HPC theta amplitude across trials for eight recordings. Two recordings were randomly chosen from each animal. Colored dots show theta amplitude envelope means for each trial and each recording chosen. Each dot is normalized to trial 1 (large, black dot) to emphasize the change in amplitude relative to trial 1. Each color represents data from one recording. The black trace represents averages across all animals for one set of chosen recordings, and the gray trace represents averages across animals for the second set of chosen recordings. All normalized means for all animals fell below the reference value for trial 1.

For each recording, t-tests were run comparing average envelope values from one trial type to all other trials types (e.g. trial 1 vs trials 2-4; trial 2 vs trials 1 and 3-4). Trial 1 theta amplitudes were significantly higher compared to trials 2-5, for seven of the eight recordings analyzed (p-values ranged from p = 4.89e-9 to p = 0.087). These figures depict a reliable shift in global activity toward enhanced theta oscillations during trial 1 that accompany increased firing rates among neurons for trial 1 as described in the previous section.

4.3.3 Spatial Tuning of Hippocampal and Parietal Neurons Aligned to the Track, as Opposed to Environmental, Space

We next examined whether HPC and PPC activity differentiated upcoming choice behavior and how this relates to the environmental space that, by the applied rule, guides choice selection. Given the block structure of the task and that trial 1 of a block is differentiated both behaviorally and neurophysiologically, firing pattern differences on track locations (1-4) were examined using trial 1 data only (figure 9).

Prior work indicates that both HPC and PPC neurons exhibit spatially-tuned firing rates in track-based environments (O'Keefe & Conway, 1978; McNaughton et al., 1983; McNaughton et al., 1994; Nitz, 2006). For open tracks, such as the one used in the current study, spatially tuned firing fields of HPC neurons (i.e., "place cells") change when the animal traverses the same route in different locations in the room, adhering to the boundaries of the experimental room space as the spatial reference frame (Alexander & Nitz, 2015). PPC firing patterns do not change, instead adhering to the route space (Nitz, 2006; Nitz, 2009). In addition, prior work on 'prospective' and 'retrospective' encoding of environmental location specifies that HPC in-field firing rates discriminate different routes taken through the same location, effectively reflecting both environmental location and the trajectory through that location (Frank et al., 2000; Wood et al., 2000; Ferbinteanu & Shapiro, 2003; Ainge et al., 2007; Nitz, 2006; Grieves et al., 2016). Therefore we would certainly expect different HPC patterns for track locations 1 versus 4 (where environmental location of the track is maximally different) as well as different HPC patterns for the different left versus right turn trajectories utilized according to the spatial/behavioral rule (e.g., track location 1 versus 3, 2 versus 3, etc.).

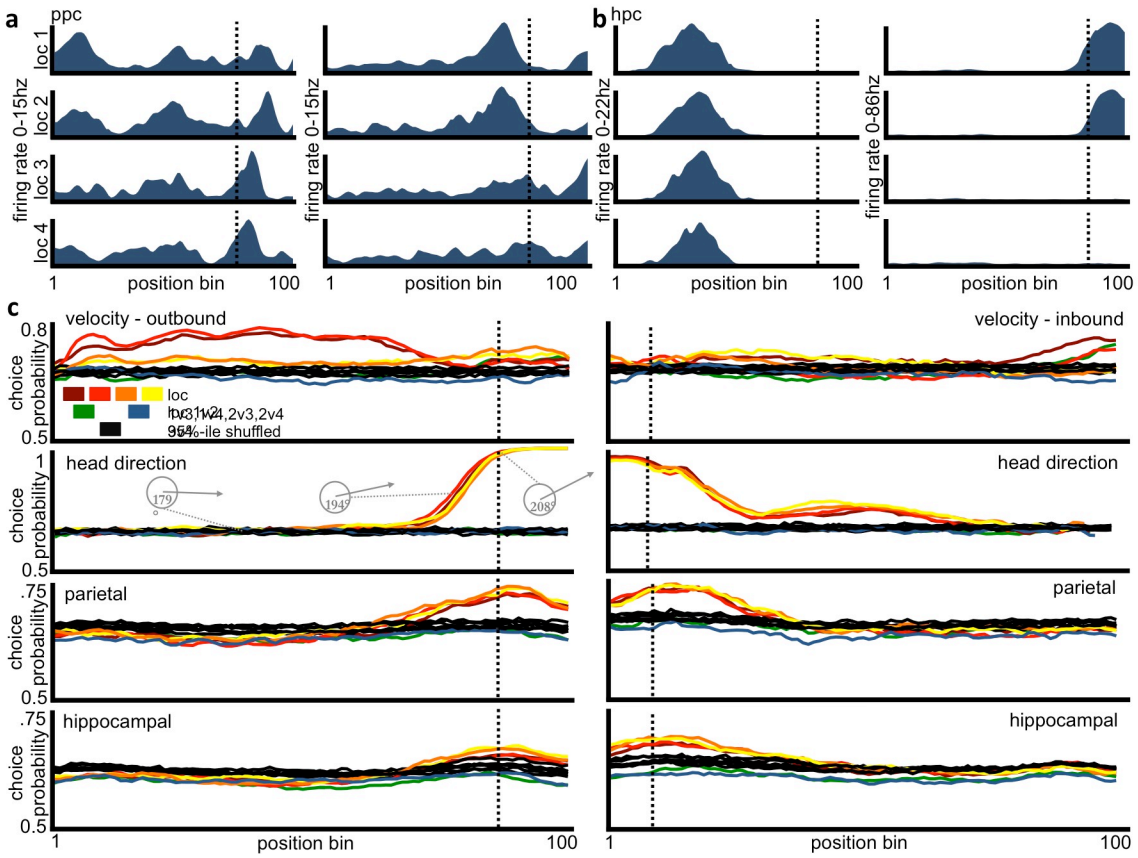

Figure 9. Choice probability analysis shows spatial tuning is aligned to track, not environment. (a-b) Outbound mean firing rates of example neurons. **(a)** Mean firing rate vectors for two example PPC neurons in each track location 1-4 (trial 1 only). Dashed line demarcates turn location. **(b)** Mean firing rate vectors for two example HPC neurons in each track location 1-4 (trial 1 only). Firing patterns anchored to track space even as the track moved to different locations in the room. It should be noted that the firing pattern for the neuron on the right followed the track space in locations 1 and 2 only, because the animal makes the opposite turn in locations 3 and 4 and ends up in a different space on the track. **(c)** Location choice probability plots. Outbound and inbound mean choice probability plots for velocity, head direction, PPC firing rates, and HPC firing rates. Warm colors represent pairwise between-fragment comparisons (location 1vs3, 2vs3, 1vs4, etc) while cool colors represent pairwise within-fragment comparisons (1vs2, 3vs4). Black lines indicate 95th percentile of choice probabilities from shuffled data. Dashed black line indicates turn location.

Paradoxically, linearized firing rate vectors of both HPC and PPC neurons follow the space of the track across multiple environmental locations of the track (1-4), similar to the pattern of the neurons depicted in figure 9a-b. It should be noted that the neuron on the right in figure 9b only fires when the track is placed in locations 1 and 2 because this

place field occurred after the turn. The turn required for locations 3 and 4 is the opposite turn from locations 1 and 2, so the location on the T-shaped track is different. Animals did not pass through this same place on the maze when turning the opposite direction for track locations 3 and 4, so this neuron did not fire here, but the firing pattern followed the track space from location 1 to location 2. Such a result is consistent with the earlier presented behavioral findings that rule out simple, independent place-choice associations as a means of solving the task. But, the spatial tuning according to the space of the track itself distinguishes the present work from most prior work and may reflect the nature of the task.

To quantify this effect across the full population of neurons, the same CP analysis used to examine trial comparisons was also used for track location comparisons (track locations 1-4; figure 9c). Essentially, the analysis asks whether HPC and/or PPC firing rates differentiate any of track locations (locations 1-4) from one another. Pairwise track location comparisons can be placed into two categories: 'within-fragment' comparisons where the firing pattern over a track location is compared to that from the same fragment (i.e., locations 1 versus 2 and 3 versus 4), and 'between-fragment' comparisons where firing patterns over track locations from separate fragment subspaces are compared (i.e., locations 1 versus 3 and 2 versus 4, etc.). Across the population, mean CP for between-fragment differentiation did not appear in PPC or HPC until the animal was actually turning (Figure 9c, black dashed lines indicate turn location). Figure 9c depicts CP for head direction on left-turning versus right-turning trajectories, revealing a bias in orientation at a point approximately 38cm prior to the front edge of the T-juncture. Inconsistent with most prior reports, neither HPC nor PPC neurons indicated choice prior

to the behavioral manifestation of the choice. Instead, the time course of firing rate differentiation between fragments maps well with the time course of head direction differentiation, the earliest behavioral indicator of the animal's choice. Essentially, we find little to no evidence for reliable encoding of upcoming choice ('prospective' information) in either brain region. Firing rate CPs also did not differentiate within-fragment track locations despite the fact that the track was moved across environmental space and despite the fact that the task demands an appreciation of position in environmental space.

We next determined whether HPC or PPC neurons differentiate track location and/or trajectory on the return or 'inbound' trips back to the base of the T-maze stem. Between-fragment differentiation was found for these inbound runs, but only for track regions near the turn site (Figure 9c). Furthermore, these differences were over regions of the track that differ in location (left versus right side of the T stem) and for which the animal's head orientation differs (Figure 9c). The results for inbound runs provide evidence that the animal may be encoding memories for the prior outbound action. Such a strategy would be consistent with trials 2-5 having near perfect choice accuracy that is significantly greater than that for trial 1.

Thus, for both inbound and outbound trajectories, mean CP values across the population yield little evidence for differentiation of track location or trajectory that cannot be explained by differences in head orientation. Yet, small differences among a large population of neurons might together yield discriminable ensemble firing patterns depending on how output from HPC and/or PPC is read by their efferent targets. To investigate ensemble differentiation within- and across-boundary, correlation matrices

were constructed for each of the pairwise location comparisons (figure 10a-b). Such matrices depict the correlations among firing patterns from the entire population of neurons for every track position bin against all others. The diagonal of such a matrix depicts correlations among firing patterns from the same track bins, but at different track locations (i.e., track locations 1-4). This yields visualization of the extent to which HPC or PPC ensembles exhibit similar firing patterns across different bins of the track (bins 1-100) and different track locations in the room (1-4). The matrices themselves are meant to be descriptive, and in this case, the ones pictured illustrate a high degree of similarity in firing within fragment (location 1vs2) as well as a high degree of similarity along the stem of the T between fragments (location 1vs4).

When considering track bins along the stem portion of the T-maze (prior to the turn), PPC ensemble correlations along the diagonal of these matrices were fairly strong (0.5-0.7) for within-fragment track location pairings (track locations 1 versus 2 and 3 versus 4) and for between-fragment track location pairings (1 versus 3, 1 versus 4, 2 versus 3, 2 versus 4). For some T-stem locations, HPC ensemble pattern correlations were somewhat stronger for within-fragment than for between-fragment track location pairings (figure 10a). Yet, for most positions, the correlation values fall within the 95% confidence intervals for a distribution of correlations taken following randomization of track location identities, illustrating a high degree of similarity across all locations. In all, the ensemble correlations for both HPC and PPC are in close agreement with the CP analyses made on single neurons. Both HPC and PPC discriminate locations along the track, but not the track locations in the environment; overall spatial tuning in both follows the frame of reference given by the track.

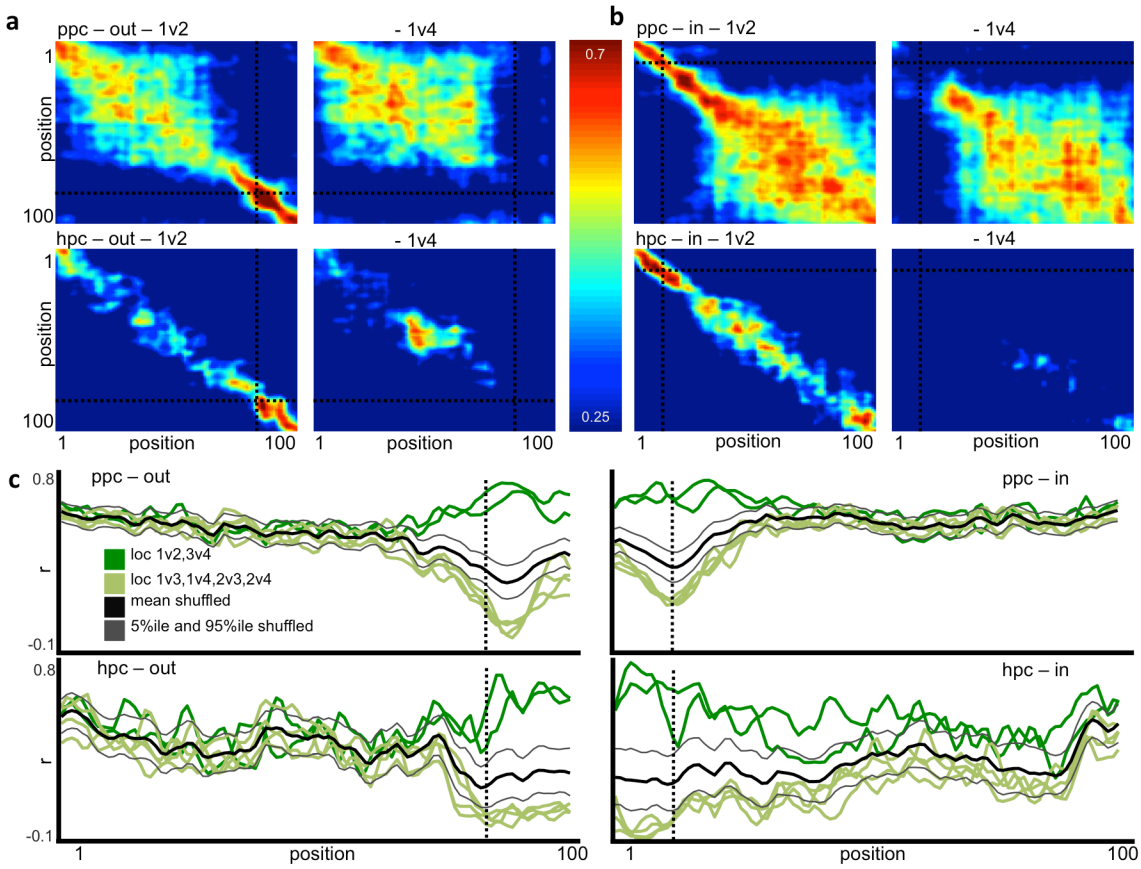

Figure 10. Ensemble correlation matrices show HPC and PPC ensembles discriminate locations along the track, but not the track locations in the environment. (a) Ensemble correlation matrices for outbound runs. Upper: Parietal correlation matrices for locations 1vs2 (left) and 1vs4 (right; within and between-fragment comparisons, respectively). Lower: Hippocampal correlation matrices for locations 1vs2 (left) and 1vs4 (right). Turn location is demarcated by dashed line. **(b)** Ensemble correlation matrices for PPC (upper) and HPC (lower) inbound runs. Left column shows within-fragment correlations (1vs2) and right column shows between-fragment correlations (1vs4). **(c)** Pairwise track location correlations across matched position bins. Left column: PPC and HPC outbound correlations of all pairwise comparisons over the same track space (diagonal of correlation matrices in a-b). Within-fragment comparisons (1vs2, 3vs4) are shown in dark green while between-fragment comparisons are shown in light green. Bold black line shows mean correlation from a distribution of shuffled data. Flanking gray lines depict 95th percentile (above) and 5th percentile (below) correlation from a distribution of shuffled data. Dashed line demarcates turn location. Right column: Correlation traces for inbound runs.

In both PPC and HPC, stronger differentiation between ensemble correlations occurred closer to the turn where differentiation in head orientation has already occurred. This finding is also in accord with the CP analysis on individual neurons. Figure 10c

plots pairwise correlations between different track locations (1-4) over the same track space (diagonals from figure 10a-b; dark green traces = within-fragment; light green traces = between-fragment), along with a mean (bold black trace), 5th percentile (lower thin gray traces), and 95th percentile (upper thin gray traces) of correlations generated after random shuffling of track location, allowing easier visual comparison of correlation matrix diagonals. Dark and light green traces did not show fragment differentiation until approaching the turn (black dashed line).

We also examined ensemble correlations of inbound runs to determine any differentiation within- or between-boundary track location pairings. In HPC, inbound, between-fragment (light green traces) differentiation occurred throughout most of the run. Ensemble patterns for inbound runs from different track locations are less alike over the entire track when those track locations are 'between-fragment' (requiring different outbound turn choices); this is true even for positions along the T-maze stem for which head orientation does not differ (figure 9c). Thus, unlike the CP analysis, the ensemble pattern observable from the correlations reveals a much greater tendency for between-fragment representations to be different as the animal returns, potentially contributing to better performance on subsequent trials by encoding memory for the prior trial. Such a finding is in line with improved behavioral accuracy on trials 2-5 of each block. We speculate that a working memory representation for the prior choice is being held during return runs so that accuracy can be improved (or sustained if already correct) on subsequent trials, and this would be consistent with other studies (Jadhav, Kemere, German, & Frank, 2012; Wang, Romani, Lustig, Leonardo, & Pastalkova, 2015). This would also suggest that the increase in HPC activity during trial 1 outbound runs supports

a short-term memory formation in which the rat holds the memory for his prior action and outcome during return runs, and can decide his next action accordingly.

4.4 Discussion

Under circumstances in which decision-making rules arbitrarily divide an environment, HPC and PPC spatial firing patterns exhibited three unexpected features that align with the choice behavior of the animals. First, spatially tuned firing rate magnitudes were augmented in HPC and modulated in PPC on the first trial of each block relative to trials 2-5. These changes parallel changes in task demands and performance accuracy from the first trial to subsequent trials of a five-trial block. In HPC, such modulation was biased toward increased firing and backward shifts in firing fields on trial 1. Second, across trial blocks with the T-maze at different environmental locations, the spatially tuned firing in both HPC and PPC shifted with the maze itself as opposed to taking the experimental room as the frame of reference. Effectively, this resulted in a shared, maze-based spatial reference frame across both environmental fragments and a highly generalized set of firing patterns across all choice locations. Third, along the T-maze stem, HPC and PPC firing patterns did not discriminate the upcoming turn choice beyond what might be expected based on differences in the animal's speed and orientation. Most, if not all, prior studies find extensive discrimination of trajectories for portions of mazes held at single environmental locations (Wood et al., 2000; Grieves et al., 2016; Ainge et al., 2007; Frank et al., 2000; Nitz, 2006; Ferbinteanu & Shapiro, 2003). Together, the results suggest a novel, shared dynamic by which HPC and cortex can interact to guide choice behavior in complex, path-based environments where correct

choice behavior varies across multiple environmental locations and as a function of recent experience.

Both HPC and PPC ensembles differentiated trial 1 of a block from subsequent trials (figure 6d). In HPC this arose by way of systematically higher firing rates and earlier onset of within-field firing on trial 1 as compared to trials 2-5 (figure 7b-f). In PPC, rate differentiation according to trial number was strong overall across the ensemble, but was not systematic in the sense of net higher or lower firing rates among the neuron population. This can be interpreted as a balanced, bi-directional rate remapping (figure 7b-c). Notably, trial differentiation is also reflected in the rats' behavior as it parallels significantly lower accuracy on trial 1 compared to subsequent trials. The trial-dependent changes in activity may reflect the extra difficulty in the first trial decision-making inherent to the structure of the task. As discussed below, this could reflect alterations in the strategy used to determine choice and/or alterations in attention, or perhaps a greater demand on retrieval mechanisms on the first trial.

The results pertaining to differences in spiking activity across trials suggest a unique strategy-based modulation of HPC and PPC dynamics. Such a robust distinction between trial 1 and trials 2-5, both behaviorally and neurophysiologically, implies two strategies are used by the rat depending on recent experience at a track location: 1) a trial 1 'track location based strategy' in which the rat needs to know its allocentric room location; and 2) a trial 2-5 'prior response strategy' in which the rat simply needs to execute the same procedure as in the prior trial, if rewarded, or the opposite procedure if not rewarded. In this respect, it is notable that ensemble firing patterns for inbound runs discriminated return-path positions along the stem, consistent with encoding of the just-

executed left-right turn choice. It is also possible that the rat has already encoded the trial 1 choice before starting the first inbound run, and that inbound activity reflects prospective planning of the next choice on trials 2-5. The prior response strategy could seemingly take advantage of such encoding of recent history, but would not require any knowledge as to room location for decision-making. Nevertheless, spatial tuning in PPC could still contribute a transformation to action-tuning, consistent with multiple reports of minority PPC neuron populations with consistent left/right turn discrimination in their firing rates (McNaughton et al., 1994; Nitz, 2006; Whitlock et al., 2012; Wilber et al., 2014).

The distinction between strategies may also reflect heightened attention or task engagement during trial 1 of a block when the track location has just been shifted. For any first trial, the rat must pay greater attention to its location in order to determine a correct turn decision as repeating the decision on the prior trial at another room location would yield only chance-level performance (50% correct). Alternatively, differences in behavioral performance and/or spiking activity on trial 1 could be due to greater taxation on retrieval mechanisms due to increased task demands or task engagement on the first trial of a block. Several findings in the literature suggest that HPC activity can track the recent history of exposure to a given environment and decision-making context. In humans, the hippocampal BOLD signal has been shown to decay over time with repeated experience on Y-maze tasks (Wimmer & Büchel, 2019). Similarly, c-FOS immunoreactivity in hippocampus tends to decay over time for animals that use a 'response' strategy, as opposed to a 'place' strategy when navigating to a reward site (Colombo et al., 2003). Overall increased firing rates among interneurons (Nitz &

McNaughton, 2004) and higher degrees of co-activity among place cells with overlapping fields (Cheng & Frank, 2008) has been shown in novel environments compared to familiar. Additionally, increased temporal coordination among place cells decays with subsequent experience (Cheng & Frank, 2008). Finally, both HPC sharp-wave ripple events and HPC phase precession of spiking relative to LFP theta-frequency oscillations are modulated by the degree of experience within single recording sessions (Jackson, Johnson, & Redish, 2006; Silva, Feng, & Foster, 2015). Each of these results is consistent with the observed trial-dependency in firing rates that we observed. The present findings therefore suggest that history-dependence in spatial tuning of HPC and PPC neurons dynamics can follow trial-by-trial variation in task demands even for familiar, learned environments

HPC theta rhythm amplitudes were significantly larger for trial 1 compared to trials 2-5, consistent with the observed firing rate increases on trial 1. Previous reports have found that theta power increases in a novel space, but such changes are also associated with changes in running speeds (Feng et al., 2015; Penley et al., 2013). Additionally, reduced theta frequency has been associated with novel environments in which the animal's running speeds are slower (Jeewajee, Lever, Burton, O'Keefe, & Burgess, 2008; Feng et al., 2015).

Changes in theta amplitude could conceivably reflect a boost in overall membrane potential of interneurons from neuromodulatory inputs. Norepinephrine applied to HPC has excitatory effects on HPC interneurons and principal cells in CA1 and dentate gyrus (DG) via beta-noradrenergic receptors (Pang & Rose, 1987). Locus coeruleus activation in vivo is associated with potentiation in population spike amplitude in DG (Klukowski

& Harley, 1984). Such noradrenergic-driven effects could enhance responses to relevant distal visual cues on the first trial of each block. Further work is needed to disentangle whether the overall shifts in population activity reflected by changes in theta-frequency LFP oscillations are induced indirectly through inputs from regions such as the septal nucleus (Petsche, Stumpf, & Gogolak, 1962; Leung, Martin, & Stewart, 1994). Regardless, the HPC spiking and LFP data together indicate that the output of HPC is intensified when task demands are higher.

Although firing rates discriminated the presence (trials 2-5) or absence (trial 1) of recent experience of choice outcome, HPC and PPC firing patterns on outbound routes followed the track space to different environmental locations. That is, the envelopes (i.e., patterns) of individual neuron firing rates across spatial bins of the track itself were largely unchanged for different track locations in the room. This result would appear to be related to the task conditions as opposed to the specific features of the recording environment; prior experimental work undertaken in the very same environment and on similarly constructed tracks found clear discrimination of track location for both HPC and retrosplenial cortex (Alexander & Nitz, 2015).

While the relevance of route position, but irrelevance of room position was expected for PPC, generalization of mapping across different environmental locations was unexpected for HPC. Prior research supports a model where HPC room-location encoding and PPC route-specific patterning would inform and guide the animal's navigational decision-making. Mapping of the animal's location relative to the boundaries of the observable environment (the experimental room in this case) is the most robust finding across many decades of investigation of spatial tuning in firing for

HPC neurons. There is also precedent for HPC cells to encode room changes on the same maze (Burke et al., 2005), analogous to the task used in the present study. Our results are in contradiction to this and indicate that our particular task reflects a fundamentally different navigational problem than for the more restricted case of a simple T-maze fixed to a location and absent a relationship to other choice point locations. However, there is precedent for at least *some* HPC neurons to maintain similar firing patterns at different locations (Tanila, Shapiro, & Eichenbaum, 1997; Siegel, Neunuebel, & Knierim, 2008), particularly in an environment when those locations occupy analogous positions in routes that share the same shape and directions of travel (Frank et al., 2000; Singer et al., 2010; Nitz, 2011). Additionally, depending on the task circumstances (i.e. passive placement of the animal vs. self-locomotion), it has been shown that head direction cells will sometimes use a local reference frame even in different room locations, and at other times use a global reference frame (Taube et al., 2013). Thus, the current results suggest that under the circumstances of the current task when multiple, independent T-juncture choices are made within a single environmental setting, the tendency for CA1 neuron spatial tuning to align to the T-maze space as opposed to the environmental space is maximal. Such environmental location independent spatial tuning in HPC would necessarily demand different models for cortico-hippocampal interaction in T-maze choice-making, a topic we return to later in this discussion.

In situations where different trajectories overlap over a shared space (as on the T-maze stem), trajectory-specific firing is encoded in conjunction with, and secondary to, firing tuned to location in the room. HPC 'place-cells' with such differential activity have been referred to as 'splitters' (Grieves et al., 2016) or as having 'prospective'

modulation of in-field firing rates (Ferbinteanu & Shapiro, 2003). While trajectory-specific spatially tuned firing is observed on inbound runs discrimination of trajectories on outbound runs was not observed in the present work despite the fact that both the room location of the track and the ultimate turn choice co-varied. One distinguishing factor associated with the present task is that the animal does not alternate on the T-maze while it remains in the same room location, as is done in many studies showing prospective coding. The present study does not have a true working memory component on the first trial of a block (only trial 1's were included in the location analyses). Although animals may carry a working memory from the previous block, it cannot be used effectively to solve the present task on trial 1. The track is shifted between blocks in a random fashion, so the animal is equally likely to be placed in a left-turning vs. a right-turning case. If the animal were operating under the assumption that he should turn in the same direction as in the previous block, his performance would be at chance levels. Our animals are all above chance performance. Working memory will only allow success on the task in trial 2 after being rewarded (or not) for trial 1. This may explain why our paradigm doesn't elicit strong prospective encoding, since only trial 1 data was included in the location analyses.

The lack of observed trajectory-encoding along the T-maze stem for PPC neurons is supported by recent work indicating that PPC discrimination of upcoming choice is secondary to heading angle, and that PPC encodes a conjunction of direction of motion, spatial position, and type of locomotor action (Krumin et al., 2018; Nitz, 2006; Wilber et al., 2014; Whitlock et al., 2012). We again note that responses to locomotor action may actually reflect postures taken by the animal during turning (Mimica et al., 2018). While

PPC has been suggested, in one study performed in virtual reality and under head restraint, to exhibit trajectory specific firing along T stems preceding T intersections (Harvey et al., 2012), other work suggests that such trajectory specificity is secondary to differences in heading angle (Krumin et al., 2018). Accordingly, our results demonstrate the timing of PPC ensemble differentiation of turn choice was directly coherent with head direction differentiation of turn choice, our first behavioral indicator of a decision (figure 9c).

In prior work on trajectory mapping and navigational decision-making for path networks with multiple intersections, 'prospective' encoding of upcoming trajectory was observed for HPC neurons at path positions shared by multiple trajectories (Ainge et al., 2007; Grieves et al., 2016) and trajectory differentiation was particularly strong if the eventual goals for multiple routes were in the same location (Grieves et al., 2016). However, in these cases, the entire turn-by-turn trajectory was known by the animal and was often executed in an uninterrupted fashion. What differentiates the current task from these others is that trials were, in the present case, segmented into distinct, unchained navigational decisions. In other words, there was no sequence of turns to be learned or encoded. Thus, one interpretation of the unexpected persistence in track-based firing patterns across environmental space and across left-going versus right-going trajectories is that HPC creates a generalizable firing pattern that maps the animal's location relative to any upcoming choice point. Across the locations of the maze in the environment, the HPC firing patterns leading to the T-maze intersection are the same, but the associated visual cues vary. Under this circumstance, and given that the only way to solve the task is by using the distal visual cues, a possible model for a solution to this task is one in which

a decision is made based on a conjunction between the ensemble HPC location-on-track encoding and different visual scenes in which location, distance, and perspective of distal visual cues all vary. The combination of these features could determine one's location in the room (see figure 11 for illustration of this model) as required to perform a correct choice. Retrosplenial cortex and/or PPC could potentially contribute to the comparison of different environmental views (of each track location) against the current encoding of track position by HPC in order to determine left-right choice. Given the large body of work finding action correlations in PPC neuron populations, it is plausible that PPC then generates a pattern of activity reflecting turn choice and outputs this to secondary motor cortex, thereby translating cognition into action (Olson et al., 2020).

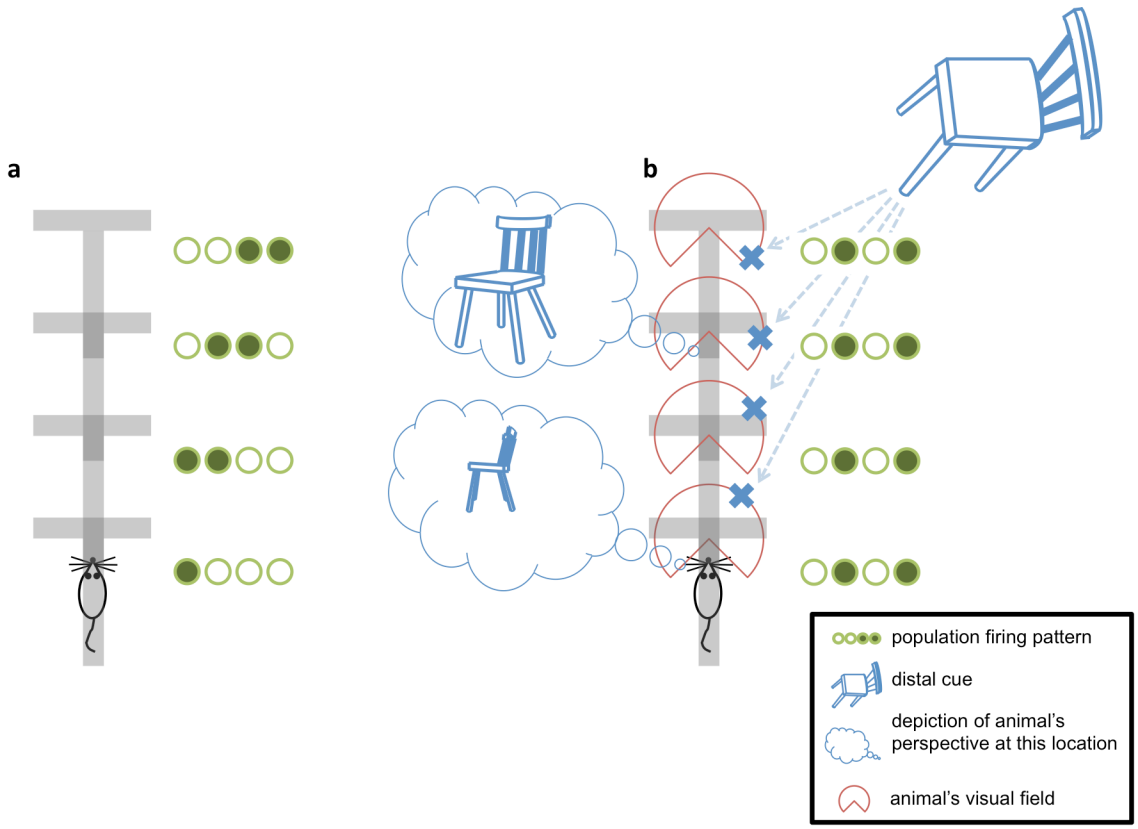

Figure 11. Schematic depicting possible decision model based on conjunction between population HPC location-on-track encoding and different visual scenes. T-shaped track laid out in track locations 1-4 is depicted in gray. The green circles represent firing patterns of the hippocampal population at the different room locations. **(a)** The population firing patterns are different at different allocentric room locations. **(b)** The population firing patterns are the same at the different room locations (consistent with the current study). The blue chair represents a distal cue in the room, and the rat's visual perspective of the cue at different room locations is depicted inside the thought bubbles. The red half circles symbolize the rat's visual field, and the blue X's show the location of the chair in the animal's field of view at the different room locations.

In summary, both HPC and PPC patterns generalize across multiple T-maze room locations and differentiate the experiential context that arises from the recent history at a location. These unexpected features are found under a navigational context in which repeated T-like intersections are encountered independently. Straight paths leading to left versus right turn choices occur regularly in both the wild and city-situated navigation where obstructions to travel are distributed throughout the space. In particular, these

scenarios frequently occur in a city with intersections organized in a regularly patterned grid. Any single intersection located within such a city has an experiential context where, upon first approach, one has to know their absolute location in the environment in order to turn correctly toward a goal. However, upon repeated approaches to the same intersection one simply has to recognize the visual cues at that intersection, and repeat what becomes a more automatic procedure. In considering not recent experience, but instead the locations of multiple T-intersections in a single, continuous environment, the present work emphasizes the importance of navigation under circumstances in which these multiple T-choices are independent as opposed to occurring in a series along a single complex trajectory (e.g., a L then R then R pattern). However, multiple intersections can be non-serially organized into neighborhoods within a city. Under these circumstances, correct decisions often cluster within neighborhoods in which to get to an area in one neighborhood (e.g. to get to the nice restaurants) one could turn right at any of the intersections, but to get to an analogous area in a different neighborhood, left turns would cluster together. Therefore the correct turn decisions themselves could define and fragment the environment based on a 'navigational rule.' The unexpected spatial tuning for HPC in the present study appears, at least, to be consistent with expression of such rule knowledge inasmuch as the animals in the present work applied the fragmentation rule robustly to novel track locations. We conclude that for complex environments in which multiple navigational decisions must be made, the context of navigation may have a strong effect on fundamental spatial tuning properties of HPC, including in-field firing rates and spatial frame of reference. The results also pave the way for future work to further identify spatial firing dynamics that reflect any of the multiple ways that division

of continuous spaces into fragments or ‘neighborhoods’ can occur (Wang, Monaco, & Knierim, 2020).

Chapters 3 and 4, in part, have been published in *Neurobiology of Learning and Memory,* Shelley, L.E., Barr, C. I., & Nitz, D.A. (2022). The author of the dissertation is the primary author of this publication.

Chapter 5: General Discussion

In the experiments discussed, we sought to examine posterior parietal and hippocampal dynamics involved in representation of complex environments and spatial tasks. Experiment 1 examined spatially specific firing patterns of HPC and PPC as they relate to movement through locations in an environment and locomotor behaviors associated with such movement. The recursion in path shape on a spiral track allowed for examining analogous locomotor actions in different room locations, and the three-dimensional aspect of the track allowed for examination of stair hopping and ramp-running behaviors. We found that PPC population activity mapped location, actions, and progress through a trajectory, and that PPC and HPC's scale of representation followed the variation in the locomotor action being performed as animals traversed the track. These results shed light on encoding of path running episodes in a way that goes beyond memory for locations visited during a trajectory and includes the locomotor actions taken along those trajectories.

Using a different paradigm, experiment 2 examined behavior associated with a complex and abstract feature of space involving dividing a room into two fragments using only a behavioral rule, absent any physical or visual dividing line. All animals very quickly learned to apply the behavioral rule at different room locations. To our knowledge, this represents the first work using decision-making rules to force an arbitrary division of an environment. In addition to the environmental fragmentation, we found lower accuracy on the first trial of a block compared to subsequent trials, which gives rise to the possibility that animals may be using different strategies on the first trial of a block, and also that the neural mapping of the space might differentiate trials.

Following the logic and paradigm used in experiment 2, experiment 3 examined both fragment and trial differentiation by PPC and HPC. Experiment 3 found three unexpected features of HPC and PPC firing patterns. First, rate magnitudes of spatially tuned firing patterns differentiated the first trial of a block compared to subsequent trials, paralleling experiment 2's poorer behavioral accuracy for trial 1. In HPC, firing rate modulation was characterized by overall increased rates and a backward-shift in the location of firing fields in trial 1. Second, HPC and PPC spatially tuned firing remained with the maze itself across environmental locations, as opposed to differentiating the different room locations (which would have been expected of HPC neurons as found in most prior work on HPC mapping), creating a maze-based spatial reference frame across both environmental fragments and all choice locations. Third, HPC and PPC firing patterns did not discriminate the upcoming turn choice while on the stem beyond what could be attributed to differences in the animal's speed and orientation between turn choices. Most, if not all, prior studies find trajectory discrimination for such portions of mazes that are at the same location, prior to (or after) a turn. We presented a model for how HPC and PPC firing patterns could lead the animal to solve the task in Experiment 3. Our interpretation is that across although HPC patterns remained stable, visual cues changed across track locations within the environment. Such pairing would map location on the track but differentiate track location and lead to a correct turn decision.

Such studies investigating HPC and PPC mapping uncover the remarkable forms by which these two networks work together to map position and actions within allocentric and egocentric frameworks. These two brain areas share some tasks but are generally complementary in their function taking spatial cognition into actions within that

space, and translating that into spatial decision-making. Experience cannot be separated from its spatial context, almost everything we experience and memory for those experiences is rooted in environmental space. The spatial and action dynamic mapping by HPC, PPC, and other related structures give rise to complex and sometimes abstract cognitive phenomena, connecting behavior and neural activity to create a cohesive cognitive experience of an event, and form the basis by which an event of moving through space is experienced and remembered.

REFERENCES

Aghajan, Z. M., Acharya, L., Moore, J. J., Cushman, J. D., Vuong, C., & Mehta, M. R. (2015). Impaired spatial selectivity and intact phase precession in two-dimensional virtual reality. *Nature Neuroscience, 18,* 121-128.

Aglioti, S., Smania, N., & Peru, A., (1999). Frames of reference for mapping tactile stimuli in brain damaged patients. *Journal of Cognitive Neuroscience, 11*(1), 67-79.

Ainge, J. A., Tamosiunaite, M., Woergoetter, F., & Dudchenko, P. A. (2007). Hippocampal CA1 place cells encode intended destination on a maze with multiple choice points. *The Journal of Neuroscience, 27,* 9769-9779.

Alexander, A. S. & Nitz, D. A. (2015). Retrosplenial cortex maps the conjunction of internal and external spaces. *Nature Neuroscience, 18,* 1143-1151.

Alexander, A. S., Rangel, L. M., Tingley, D., & Nitz, D. A. (2018). Neurophysiological signatures of temporal coordination between retrosplenial cortex and the hippocampal formation. *Behavioral Neuroscience, 132,* 453-468.

Andersen, R. A., Essick, G. K., & Siegel, R. M. (1985). Encoding of spatial location by posterior parietal cortex neurons. *Science, 230*(4724), 456-458.

Avillac, M., Deneve, S., Olivier, E., Pouget, A., & Duhamel, J. R. (2005). Reference frames for representing visual and tactile locations in parietal cortex. *Nature Neuroscience, 8*(7), 941-949.

Benoit, R. G. & Schacter, D. L. (2015). Specifying the core network supporting episodic simulation and episodic memory by activation likelihood estimation. *Neuropsychologia, 75,* 450-457.

Bi, G. & Poo, M. (2001). Synaptic modification by correlated activity: Hebb's postulate revisited. *Annual Reviews Neuroscience, 24,* 139-166.

Bonner, M. F., & Epstein, R. A. (2017). Coding of navigational affordances in the human visual system. *PNAS, 114*(18), 4793-4798.

Britten, K. H., Newsome, W. T., Shadlen, M. N., Celebrini, S., & Movshon, J. A. (1996). A relationship between behavioral choice and the visual responses of neurons in macaque MT. *Visual Neuroscience, 13*(1), 87-100.

Burke, S. N., Chawla, M. K., Penner, M. R., Crowell, B. E., Worley, P. F., Barnes, C. A., & McNaughton, B. L. (2005). Differential encoding of behavior and spatial context in deep and superficial layers of the neocortex. *Neuron, 45,* 667-674.

Burwell, R. D. (2000). The parahippocampal region: Corticocortical connectivity. *Annals New York Academy of Sciences, 911,* 25-42.

Casali, G., Bush, D., & Jeffery, K. (2019). Altered neural odometry in the vertical dimension. *PNAS, 116,* 4631-4636.

Chang, Q. & Gold, P. E. (2003). Switching memory systems during learning: Changes in patterns of brain acetylcholine release in the hippocampus and striatum in rats. *The Journal of Neuroscience, 23*(7), 3001-3005.

Cheng, S. & Frank, L. M. (2008). New experiences enhance coordinated neural activity in the hippocampus. *Neuron, 57*(2), 303-313.

Cohen, Y. E. & Andersen, R. A. (2002). A common reference frame for movement plans in the posterior parietal cortex. *Nature Reviews Neuroscience, 3*, 553-562.

Colombo, P. J., Brightwell, J. J., & Countryman, R. A. (2003). Cognitive strategy-specific increases in phosphorylated cAMP response element-binding protein and c-Fos in the hippocampus and dorsal striatum. *The Journal of Neuroscience, 23*(8), 3547-3554.

Cowen, S. L. & Nitz, D. A. (2014). Repeating firing fields of CA1 neurons shift forward in response to increasing angular velocity. *The Journal of Neuroscience, 34,* 232-241.

Crowe, D. A., Averbeck, B. B., & Chafee, M. V. (2010). Rapid sequences of population activity patterns dynamically encode task-critical spatial information in parietal cortex. *The Journal of Neuroscience, 30,* 11640-11653.

Dabaghian, Y., Brandt, V. L., & Frank, L. M. (2014). Reconceiving the hippocampal map as a topological template. *eLife,* 3, e03476.

Dragoi, G. & Buzsáki, G. (2006). Temporal encoding of place sequences by hippocampal cell assemblies. *Neuron, 50*(1), 145-157.

Driver, J. & Mattingley, J. B. (1998). Parietal neglect and visual awareness. *Nature Neuroscience, 1,* 17-22.

Duhamel, J. R., Colby, C. L., & Goldberg, M. E. (1998). Ventral intraparietal area of the macaque: Congruent visual and somatic response properties. *Journal of Neurophysiology, 79,* 126-136.

Ergorul, C. & Eichenbaum, H. (2004). The hippocampus and memory for "what," "where," and "when." *Learning & Memory, 11,* 397-405.

Feng, T., Silva, D., & Foster, D. J. (2015). Dissociation between the experience-dependent development of hippocampal theta sequences and single-trial phase precession. *The Journal of Neuroscience, 35*(12), 4890-4902.

Ferbinteanu J. & Shapiro, M. L. (2003). Prospective and retrospective memory coding in the hippocampus. *Neuron, 40,* 1227-1239.

Frank, L. M., Brown, E. N., & Wilson, M. (2000). Trajectory encoding in the hippocampus and entorhinal cortex. *Neuron, 27,* 169-178.

Freedman, D.J. & Assad, J.A. (2006). Experience-dependent representation of visual categories in parietal cortex. *Nature, 443,* 85-88.

Grieves, R. M., Wood, E. R., & Dudchenko, P. A. (2016). Place cells on a maze encode routes rather than destinations. *eLife, 5,* e15986.

Grunewald, A., Linden, J. F., & Andersen, R. A. (1999). Responses to auditory stimuli in macaque lateral intraparietal area. I. Effects of training. *Journal of Neurophysiology, 82*(1), 330-342.

Gupta, A. S., van der Meer, M. A., Touretzky, D. S. & Redish, A. D. (2012). Segmentation of spatial experience by hippocampal theta sequences. *Nature Neuroscience, 15,* 1032-1039.

Hafting, T., Fyhn, M., Molden, S., Moser, M. B., & Moser, E. I. (2005). Microstructure of a spatial map in the entorhinal cortex. *Nature, 436,* 801-806.

Harvey, C. D., Coen, P., & Tank, D. W. (2012). Choice-specific sequences in parietal cortex during a virtual-navigation decision task. *Nature, 484*(7392), 62-68.

Hassabis, D., Kumaran, D., & Maguire, E. A. (2007). Using imagination to understand the neural basis of episodic memory. *The Journal of Neuroscience, 27,* 14365-14374.

Hayman, R., Casali, G., Wilson, J. J., & Jeffery, K. J. (2015). Grid cells on steeply sloping terrain: Evidence for planar rather than volumetric encoding. *Frontiers in Psychology, 6,* 925.

Hayman, R., Verriotis, M., Jovalekic, A., Fenton, A. A., & Jeffery, K. J. (2011). Anisotropic encoding of three-dimensional space by place cells and grid cells. *Nature Neuroscience, 14,* 1182-1188.

Hirtle, S.C. & Jonides, J. (1985). Evidence of hierarchies in cognitive maps. *Memory & Cognition, 13*(3), 208-217.

Huerta, P. T. & Lisman, J. E. (1993). Heightened synaptic plasticity of hippocampal CA1 neurons during a cholinergically induced rhythmic state. *Nature, 364,* 723-725.

Jackson, J. C., Johnson, A., & Redish, A. D. (2006). Hippocampal sharp waves and reactivation during awake states on repeated sequential experience. *The Journal of Neuroscience, 26*(48), 12415-12426.

Jadhav, S. P., Kemere, C., German, P. W., & Frank, L. M. (2012). Awake hippocampal sharp-wave ripples support spatial memory. *Science, 336*(6087), 1454-1458.

Javadi, A. H., Emo, B., Howard, L. R., Zisch, F. E., Yu, Y., Knight, R., . . . Spiers, H. J. (2017). Hippocampal and prefrontal processing of network topology to simulate the future. *Nature Communications,* 8, 14652.

Jeewajee, A., Lever, C., Burton, S., O'Keefe, J., & Burgess, N. (2008). Environmental novelty is signaled by reduction of the hippocampal theta frequency. *Hippocampus, 18*(4), 340-348.

Karnath, H. O., Christ, K., & Hartje, W. (1993). Decrease of contralateral neglect by neck muscle vibration and spatial orientation of trunk midline, *Brain, 116,* 383-396.

Kjelstrup, K. B., Solstad, T., Brun, V. H., Hafting, T., Leutgeb, S., Witter, M. P., . . . Moser, M. B. (2008). Finite scale of spatial representation in the hippocampus. *Science, 321,* 140-143.

Klukowski, G. & Harley, C. W. (1984). Locus coeruleus activation induces perforant path-evoked population spike potentiation in the dentate gyrus of awake rat. *Experimental Brain Research, 102*(1), 165-170.

Knierim, J. J. & McNaughton, B. L. (2001). Hippocampal place-cell firing during movement in three-dimensional space. *J Neurophysiol., 85,* 105-116.

Kolb, B. & Walkey, J. (1987). Behavioural and anatomical studies of the posterior parietal cortex in the rat. *Behavioural Brain Research, 23*, 127-145.

Kosslyn, S. M., Pick, H. L. & Fariello, G. R. (1974). Cognitive maps in children and men. *Child Development, 45*(3), 707-716.

Krumin, M., Lee, J. J., Harris, K. D., & Carandini, M. (2018). Decision and navigation in mouse parietal cortex. *eLife, 7,* e42583.

LaChance, P. A., Dumont, J. R., Ozel, P., Marcroft, J. L., & Taube, J. S. (2020). Commutative properties of head direction cells during locomotion in 3D: Are all routes equal? *The Journal of Neuroscience, 40,* 3035-3051.

Leung, L. S., Martin, L. A., & Stewart, D. J. (1994). Hippocampal theta rhythm in behaving rats following ibotenic acid lesion of the septum. *Hippocampus, 4*(2), 136-147.

Linden, J. F., Grunewald, A., & Andersen, R. A. (1999). Responses to auditory stimuli in macaque lateral intraparietal area. II. Behavioral modulation. *Journal of Neurophysiology, 82*(1), 343-358.

Lubenov, E. V. & Siapas, A. G. (2009). Hippocampal theta oscillations are travelling waves. *Nature, 459*(7246), 534-539.

Markus, E. J., Qin, Y. L., Leonard, B., Skaggs, W. E., McNaughton, B. L., & Barnes, C. A. (1995). Interactions between location and task affect the spatial and directional firing of hippocampal neurons. *The Journal of Neuroscience, 15,* 7079-7094.

Maurer, A. P., VanRhoads, S. R., Sutherland, G. R., Lipa, P., & McNaughton, B. L. (2005). Self-motion and the origin of differential spatial scaling along the septo-temporal axis of the hippocampus. *Hippocampus, 15,* 841-852.

McNamara, T.P. (1986). Mental representations of spatial relations. *Cognitive Psychology, 18*(1), 87-121.

McNaughton, B. L., Barnes, C. A., & O'Keefe, J. (1983). The contributions of position, direction, and velocity to single unit activity in the hippocampus of freely-moving rats. *Experimental Brain Research, 52,* 41-49.

McNaughton, B. L., Mizumori, S. J., Barnes, C. A., Leonard, B. J., Marquis, M., & Green, E. J. (1994). Cortical representation of motion during unrestrained spatial navigation in the rat. *Cerebral Cortex, 4,* 27-39.

Mimica, B., Dunn, B. A., Tombaz, T., Bojja, V., & Whitlock, J. R. (2018). Efficient cortical coding of 3D posture in freely behaving rats. *Science, 362,* 584-589.

Monaco, J. D., Rao, G., Roth, E. D., & Knierim, J. J. (2014). Attentive scanning behavior drives one-trial potentiation of hippocampal place fields. *Nature Neuroscience, 17*, 725-731.

Morris, R. G., Garrud, P., Rawlins, J. N. P., & O'Keefe, J. (1982). Place navigation in impaired rats with hippocampal lesions. *Nature, 297*, 681-683.

Muller, R. U. & Kubie, J. L. (1987). The effects of changes in the environment on the spatial firing of hippocampal complex-spike cells. *The Journal of Neuroscience, 7,* 1951-1968.

Newcombe, N. & Liben, L. S. (1982). Barrier effects in the cognitive maps of children and adults. *Journal of Experimental Child Psychology, 34,* 46-58.

Nitz, D. A. (2006). Tracking route progression in the posterior parietal cortex. *Neuron, 49,* 747-756.

Nitz, D. A. (2009). Parietal cortex, navigation, and the construction of arbitrary reference frames for spatial information. *Neurobiology of Learning and Memory, 91*(2), 179-185.

Nitz, D. A. (2011). Path shape impacts the extent of CA1 pattern recurrence both within and across environments. *J Neurophysiol, 105,* 1815-1824.

Nitz, D. A. (2012). Spaces within spaces: Rat parietal cortex neurons register position across three reference frames. *Nature Neuroscience, 15,* 1365-1367.

Nitz, D. A. (2013). The posterior parietal cortex: Interface between maps of external spaces and the generation of action sequences. In D. Derdikman & J. Knierim (Eds.), *Space, Time and Memory in the Hippocampal Formation*.

Nitz, D. A. & McNaughton, B. L. (2004). Differential modulation of CA1 and dentate gyrus interneurons during exploration of novel environments. *J. Neurophysiol., 91*(2), 863-872.

O'Keefe, J. O. & Conway, D. H. (1978). Hippocampal place units in the freely moving rat: Why they fire where they fire. *Experimental Brian Research, 31*(4), 573-590.

O'Keefe, J. & Dostrovsky, J. (1971). The hippocampus as a spatial map. Preliminary evidence from unit activity in the freely-moving rat. *Brain Research, 34,* 171-175.

O'Keefe, J. & Recce, M. L. (1993). Phase relationship between hippocampal place units and the EEG theta rhythm. *Hippocampus, 3,* 317-330.

Olsen, G. M., Ohara, S., Iijima, T., & Witter, M. P. (2017). Parahippocampal and retrosplenial connections of rat posterior parietal cortex. *Hippocampus, 27,* 335-358.

Olson, J. M., Li, J. K., Montgomery, S. E., & Nitz, D. A. (2020). Secondary motor cortex transforms spatial information into planned action during navigation. *Current Biology, 30*(10), 1845-1854.

Packard, M. G. (1999). Glutamate infused posttraining into the hippocampus or caudate-putamen differentially strengthens place and response learning. *PNAS, 96*(22), 12881-12886.

Packard, M. G. & McGaugh, J. L. (1996). Inactivation of hippocampus or caudate nucleus with lidocaine differentially affects expression of place and response learning. *Neurobiology of learning and memory, 65*, 65-72.

Pang, K. & Rose, G. M. (1987). Differential effects of neorepinephrine on hippocampal complex-spike and θ-neurons. *Brain Research, 425*(1), 146-158.

Pastalkova, E., Itskov, V., Amarasingham, A., & Buzsáki, G. (2008). Internally generated cell assembly sequences in the rat hippocampus. *Science, 321*(5894), 1322-1327.

Pavlides, C., Greenstein, Y. J., Grudman, M., & Winson, J. (1988). Long-term potentiation in the dentate gyrus is induced preferentially on the positive phase of theta-rhythm. *Brain Research, 439,* 383-387.

Paxinos, G. & Watson, C. *The Rat Brain in Stereotaxic Coordinates* 6th edn. (Academic Press, London, 2007).

Penley, S. C., Hinman, J. R., Long, L. L., Markus, E. J., Escabí, M. A., & Chrobak, J. J. (2013). Novel space alters theta and gamma synchrony across the longitudinal axis of the hippocampus. *Frontiers in Systems Neuroscience, 7,* 20.

Petsche, H., Stumpf, C., & Gogolak, G. (1962). The significance of the rabbit's septum as a relay station between the midbrain and the hippocampus I. The control of hippocampus arousal activity by the septum cells. *Electroencephalography and Clinical Neurophysiology, 14,* 202-211.

Porter, B. S., Schmidt, R., & Bilkey, D. K. (2018). Hippocampal place cell encoding of sloping terrain. *Hippocampus, 28,* 767-782.

Pouget, A. & Driver, J. (2000). Relating unilateral neglect to the neuronal coding of space. *Current Opinion in Neurobiology, 10,* 242-249.

Qin, Y. L., McNaughton, B. L., Skaggs, W. E., & Barnes, C. A. (1997). Memory reprocessing in corticocortical and hippocampocortical neuronal ensembles. *Phil Trans R Soc Lond B, 352,* 1525-1533.

Reep, R. L., Chandler, H. C. King, V., & Corwin, J. V. (1994). Rat posterior parietal cortex: Topography of corticocortical and thalamic connections. *Experimental Brain Research, 100*, 67-84.

Rogers, J. L. & Kesner, R. P. (2007). Hippocampal-parietal cortex interactions: Evidence from a disconnection study in the rat. *Behavioral Brain Research, 179,* 19-27.

Saj, A., Fuhrman, O., Vuilleumier, P., & Boroditsky, L. (2014). Patients with left spatial neglect also neglect the "left side" of time. *Psychological Science, 25,* 207-214.

Save, E., Paz-Villagran, V., Alexinsky, T., & Poucet, B. (2005). Functional interaction between the associative parietal cortex and hippocampal place cell firing in the rat. *European Journal of Neuroscience, 21*(2), 522-530.

Scoville, W. B. & Milner B. (1957). Loss of recent memory after bilateral hippocampal lesions. *J Neurol Neurosurg & Psychiat., 20,* 11-21.

Siegel, J. J., Neunuebel, J. P., & Knierim, J. J. (2008). Dominance of the proximal coordinate frame in determining the locations of hippocampal place cell activity during navigation. *J. Neurophysiol., 99*(1), 60-76.

Silva, D., Feng, T., & Foster, D. J. (2015). Trajectory events across hippocampal place-cells require previous experience. *Nature Neuroscience, 18*(12), 1772-1779.

Singer, A. C., Karlsson, M. P., Nathe, A. R., Carr, M. F., & Frank, L. M. (2010). Experience-dependent development of coordinated hippocampal spatial activity representing the similarity of related locations. *The Journal of Neuroscience, 30,* 11586-11604.

Sirota, A., Montgomery, S., Fujisawa, S., Isomura, Y., Zugaro, M., & Buzsáki, G. (2008). Entrainment of neocortical neurons and gamma oscillations by the hippocampal theta rhythm. *Neuron, 60,* 683-697.

Skaggs, W. E., McNaughton, B. L., Wilson, M. A., & Barnes, C. A. (1996). Theta phase precession in hippocampal neuronal populations and the compression of temporal sequences. *Hippocampus, 6,* 149-172.

Stevens, A. & Coupe, P. (1978). Distortions in judge spatial relations. *Cognitive Psychology, 10*(4), 422-437.

Tanila, H., Shapiro, M. L., & Eichenbaum, H. (1997). Discordance of spatial representation in ensembles of hippocampal place cells. *Hippocampus, 7,* 613-623.

Taube, J. S., Muller, R. U., & Ranck, J. B. Jr. (1990). Head direction cells recorded from the postsubiculum in freely moving rats. II. Effects of environmental manipulations. *Journal of Neuroscience, 10*(2), 436-447.

Taube, J. S., Wang, S. S., Kim, S. Y., & Frohardt, R. J. (2013). Updating of the spatial reference frame of head direction cells in response to locomotion in the vertical plane. *J Neurophysiol., 109,* 873-888.

Tolman, E. C. (1948). Cognitive maps in rats and men. *The Psychological Review, 55*(4), 189-208.

Tolman, E. C., Ritchie, B. F., & Kalish, D. (1946). Studies in spatial learning; Place learning versus response learning. *Journal of Experimental Psychology, 36*, 221-229.

Tolman E. C., Ritchie, B. F., & Kalish, D. (1947). Studies in spatial learning; Response learning vs. place learning by the non-correction method. *Journal of Experimental Psychology, 37*(4), 285-292.

Vuilleumier, P., Valenza, N., Mayer, E., Perrig, S., & Landis, T. (1999). To see better to the left when looking more to the right: Effects of gaze direction and frames of spatial

coordinates in unilateral neglect. *Journal of the International Neuropsychological Society, 5*(1), 75-82.

Warren, W. H., Rothman, D. B., Schnapp, B. H., & Ericson J. D. (2017). Wormholes in virtual space: From cognitive maps to cognitive graphs. *Cognition, 166,* 152-163.

Wang, C.H., Monaco, J. D., & Knierim, J. J. (2020). Hippocampal place cells encode local surface-texture boundaries. *Current Biology, 30*(8), 1397-1409.

Wang, Y., Romani, S., Lustig, B., Leonardo, A., & Pastalkova, E. (2015). Theta sequences are essential for internally generated hippocampal firing fields. *Nature Neuroscience, 18*(2), 282-288.

Whitlock, J. R., Pfuhl, G., Dagslott, N., Moser, M. B., & Moser, E. I. (2012). Functional split between parietal and entorhinal cortices in the rat. *Neuron, 73,* 789-802.

Wiener, J. M., Ehbauer, N. N., & Mallot, H. A. (2009). Planning paths to multiple targets: Memory involvement and planning heuristic in spatial problem solving. *Psychological Research, 73,* 644-658.

Wilber, A. A., Clark, B. J., Forster, T. C., Tatsuno, M., & McNaughton, B. L. (2014). Interaction of egocentric and world-centered reference frames in the rat posterior parietal cortex. *The Journal of Neuroscience, 34,* 5431-5446.

Wimmer, G. E. & Büchel, C. (2019). Learning of distant state predictions by the orbitofrontal cortex in humans. *Nature Communications, 10*(1)*,* 2554

Witter, M. P., Naber, P. A., van Haeften, T., Machielsen, W. C. M., Rombouts, S. A. R. B., Barkhof, F., . . . Lopes da Silva, F. H. (2000). Cortico-hippocampal communication by way of parallel parahippocampal-subicular pathways. *Hippocampus, 10,* 398-410.

Wood, E. R., Dudchenko, P. A., Robitsek, R. J., & Eichenbaum, H. (2000). Hippocampal neurons encode information about different types of memory episodes occurring in the same location. *Neuron, 27,* 623-633.

Wyss, J. M & Van Groen, T. (1992). Connections between the retrosplenial cortex and the hippocampal formation in the rat: A review. *Hippocampus, 2,* 1-12.

Yamawaki, N., Radulovic, J., & Shepherd, G. M. (2016). A corticocortical circuit directly links retrosplenial cortex to M2 in the mouse. *The Journal of Neuroscience, 36*(36), 9365-9374.